Molecular Pharmacology Fast Forward. Published on October 11, 2012 as doi:10.1124/mol.112.080986
This article has not been copyedited and formatted. The final version may differ from this version.

MOL #80986

Neurounina-1, a novel compound that increases Na^+/Ca^{2+} exchanger activity, effectively protects against stroke damage

Pasquale Molinaro, Maria Cantile, Ornella Cuomo, Agnese Secondo, Anna Pannaccione, Paolo Ambrosino, Giuseppe Pignataro, Ferdinando Fiorino, Beatrice Severino, Elena Gatta, Maria José Sisalli, Marco Milanese, Antonella Scorziello, Giambattista Bonanno, Mauro Robello, Vincenzo Santagada, Giuseppe Caliendo, Gianfranco Di Renzo, Lucio Annunziato

Division of Pharmacology, Department of Neuroscience, School of Medicine, "Federico II" University of Naples-National Institute of Neuroscience, Via S. Pansini 5, 80131, Naples, Italy (P.M., M.C., O.C., A.Se., A.P., P.A., G.P., M.J.S., A.Sc., G.D.R., L.A.)
Department of Pharmaceutical and Toxicological Chemistry, Faculty of Pharmacy, "Federico II" University of Naples, Via Domenico Montesano 49, 80131, Naples, Italy (F.F., B.S., V.S., G.C.).
Department of Physics, University of Genoa, Via Dodecaneso 33, 16146 Genoa, Italy (E.G., M.R.).
Department of Experimental Medicine, Section of Pharmacology and Toxicology, University of Genoa, 16148 Genoa, Italy (M.M., G.B).

Molecular Pharmacology Fast Forward. Published on October 11, 2012 as DOI: 10.1124/mol.112.080986
This article has not been copyedited and formatted. The final version may differ from this version.

MOL #80986

Running title:
Neurounina-1 increases NCX activity and protects against stroke

Corresponding author: Prof. Lucio Annunziato, MD
Division of Pharmacology, Department of Neuroscience, School of Medicine, University of Naples "Federico II", Via Pansini 5, 80131 Naples, Italy
lannunzi@unina.it
Phone: +39-0817463318
Fax: +39-0817463323

Text pages=48
Tables=1
Figures=8
References=60
Abstract (words)=247
Introduction (words)=745
Discussion (words)=1495

Abbreviations: NCX= Na^+/Ca^{2+} exchanger; BHK= baby hamster kidney; NMDG= N-Methyl D-glucamine, TTX= tetrodotoxin; MTT= 3[4,5-dimethylthiazol-2-y1]-2,5-diphenyltetrazolium bromide; SN6= 2-[4-(4-nitrobenzyloxy)benzyl]thiazolidine-4-carboxylic acid ethyl ester; KB-R7943= 2-[2-[4-(4-nitrobenzyloxyl)phenyl]ethyl]isothiourea methanesulfonate; SEA0400= 2-[4-[(2,5-difluorophenyl)methoxy]phenoxy]-5-ethoxyaniline; YM-244769= *N*-(3-aminobenzyl)-6-[4-[(3-fluorobenzyl)oxy]-phenoxy]nicotinamide; $GABA_A$= γ-aminobutyric acid receptor A.

Molecular Pharmacology Fast Forward. Published on October 11, 2012 as DOI: 10.1124/mol.112.080986
This article has not been copyedited and formatted. The final version may differ from this version.

ABSTRACT

Previous studies have demonstrated that the knock-down or knock-out of the three Na^+/Ca^{2+} exchanger (NCX) isoforms, NCX1, NCX2 and NCX3, worsens ischemic brain damage. This suggests that the activation of these antiporters exerts a neuroprotective action against stroke damage. However, drugs able to increase the activity of NCXs are not yet available**.** We have here succeeded in synthesizing a new compound, named neurounina-1 (7-nitro-5-phenyl-1-(pyrrolidin-1-ylmethyl)-1*H*-benzo[e][1,4]diazepin-2(3*H*)-one), provided with an high lipophilicity index and able to increase NCX activity. Ca^{2+}-radiotracer, Fura-2-microfluorimetry, and patch-clamp techniques revealed that neurounina-1 stimulated NCX1 and NCX2 activities with an EC_{50} in the picomolar-low-nanomolar range, whereas it did not affect NCX3 activity. Furthermore, by using chimera strategy and site-directed mutagenesis, three specific molecular determinants of NCX1 responsible for neurounina-1 activity were identified in the α–repeats. Interestingly, NCX3 became responsive to neurounina-1 when both α–repeats were replaced with the corresponding regions of NCX1. *In vitro* studies showed that 10nM neurounina-1 reduced cell death of primary cortical neurons exposed to oxygen-glucose deprivation followed by reoxygenation. Moreover, *in vitro,* neurounina-1 also reduced GABA release, enhanced $GABA_A$-currents, and inhibited both glutamate release and NMDA receptors. More important, neurounina-1 proved to have a wide therapeutic window *in vivo*. Indeed, when administered i.p. at doses ranging 0.003-30 μg/kg, it was able to reduce the infarct volume of mice subjected to transient middle cerebral artery occlusion even up to 3-5h after stroke onset. Collectively, the present study shows that neurounina-1 exerts a remarkable neuroprotective effect during stroke and increases NCX1 and NCX2 activities.

Molecular Pharmacology Fast Forward. Published on October 11, 2012 as DOI: 10.1124/mol.112.080986
This article has not been copyedited and formatted. The final version may differ from this version.

INTRODUCTION

The Na^+/Ca^{2+} exchanger (NCX) is an important bi-directional plasmamembrane transporter that is driven by electrochemical gradient. Under physiological conditions, it mainly works in the forward mode by coupling the extrusion of one Ca^{2+} ion with the influx of three Na^+ ions into the cells. Under certain physiological and pathophysiological conditions, when the electrochemical gradient reverts, NCX works in the reverse mode, thus coupling the extrusion of three Na^+ ions with the influx of one Ca^{2+} ion (Annunziato et al.,2004;Blaustein and Lederer,1999;Philipson and Nicoll,2000).

NCX belongs to a multigene family comprising three isoforms, named NCX1, NCX2, and NCX3, which are differentially distributed through the body. NCX1 is ubiquitously expressed in all tissues, NCX2 is mainly restricted to the brain, and NCX3 is expressed exclusively in brain and skeletal muscles (Quednau et al.,1997). These NCX isoforms have similar molecular topologies comprising nine transmembrane segments and a large cytoplasmatic loop that regulates their activity (Nicoll et al.,1999). All NCX isoforms share two highly conserved repeat sequences, named α_1 and α_2, that are involved in the ionic transport process (Nicoll et al.,1996).

The primary function of NCX is to extrude Ca^{2+} from the cell, in the forward mode, using $[Na^+]$ gradient. However, under some physiological conditions, such as the occurrence of an action potential or of spontaneous $[Ca^{2+}]_i$ oscillations, NCX could revert its mode of operation, thus participating to ER-Ca^{2+} refilling. In fact, it has been recently demonstrated that spontaneous $[Ca^{2+}]_i$ oscillations induced by IP_3-receptor stimulation might lead to the activation of non-selective cation channels, that causes Na^+ influx into the junctional cytosol microdomains. This influx facilitates the entrance of Ca^{2+} through NCX working in the reverse mode (Fameli et al.,2007). On the other hand, under pathological conditions, the function of NCX is more complex. More specifically, in the early phase of neuronal

Molecular Pharmacology Fast Forward. Published on October 11, 2012 as DOI: 10.1124/mol.112.080986
This article has not been copyedited and formatted. The final version may differ from this version.

anoxic insult, the Na^+/K^+-ATPase blockade increases $[Na^+]_i$ which in turn induces NCX to reverse its mode of operation. Although during this phase NCX causes an increase in $[Ca^{2+}]_i$, its effect on neurons appears beneficial for two reasons. First, by promoting Ca^{2+}-influx, NCX favors Ca^{2+}-refilling into the endoplasmatic reticulum (ER), which is depleted by anoxia followed by reoxygenation, thus allowing neurons to delay ER stress (Sirabella et al.,2009). Second, by eliciting the decrease in $[Na^+]_i$ overload, NCX prevents cell swelling and death (Annunziato et al.,2007). Conversely, in the later phase of neuronal anoxia, when $[Ca^{2+}]_i$ overload takes place, NCX forward mode of operation contributes to the lowering of $[Ca^{2+}]_i$, thus protecting neurons from $[Ca^{2+}]_i$-induced neurotoxicity (Annunziato et al.,2004). Furthermore, NCX is involved in some serious diseases characterized by a loss of ion homeostasis control, including Alzheimer's disease, multiple sclerosis, and epilepsy (Craner et al.,2004;Ketelaars et al.,2004;Pannaccione et al.,2012). Recently, experiments in ischemic rats treated with inhibitors of NCX activity or synthesis, together with experiments in knock-out mice for *ncx2* or *ncx3* gene, have demonstrated that the blockade of NCX protein synthesis or activity worsens ischemic brain damage by dysregulating Na^+ and Ca^{2+} homeostasis (Jeon et al.,2008;Molinaro et al.,2008;Pignataro et al.,2004a;Pignataro et al.,2004b). Therefore, in the last years, a great interest has been devoted to the identification of new compounds capable to increase NCX activity to limit the extension of ischemic brain damage (Annunziato et al.,2009). To date, only NCX inhibitors are available including CB-DMB (Secondo et al.,2009), KB-R7943 (Watano et al.,1999), SEA0400 (Matsuda et al.,2001), SM-15811 (Hasegawa et al.,2003), SN-6 (Iwamoto et al.,2004a), and YM-244769 (Iwamoto and Kita,2006). These inhibitors have a number of interesting features**.** In particular, KB-R7943 preferentially inhibits NCX3 more than NCX1 and NCX2 (Iwamoto et al.,2001), whereas SEA0400 and SN-6 preferentially block NCX1 rather than NCX2 and NCX3 (Iwamoto et al.,2004a; Iwamoto et al.,2004b).

Molecular Pharmacology Fast Forward. Published on October 11, 2012 as DOI: 10.1124/mol.112.080986
This article has not been copyedited and formatted. The final version may differ from this version.

However, despite their potency, these compounds possess some non-specific actions against other ion channels and receptors (Pintado et al.,2000;Reuter et al.,2002).

To obtain an activator of the NCX isoforms, we modified the structure of one of the most potent NCX inhibitors, SM-15811, thereby synthesizing a new compound, 7-nitro-5-phenyl-1-(pyrrolidin-1-ylmethyl)-1*H*-benzo[e][1,4]diazepin-2(3*H*)-one, that we named neurounina-1. In the present paper, we investigated the effect of this newly synthesized compound on NCX1, NCX2, and NCX3 activity in the forward and reverse modes of operation by means of Ca^{2+}-radiotracer, Fura-2 microfluorimetry, and patch-clamp techniques, and thereafter, with the help of chimera strategy, deletion and site-directed mutagenesis, we identified the molecular determinants of this compound on NCX structure.

More important, since NCX activity is involved in stroke pathophysiology, we examined the putative protective effects of neurounina-1 on *in vitro* and *in vivo* models of cerebral ischemia.

Molecular Pharmacology Fast Forward. Published on October 11, 2012 as DOI: 10.1124/mol.112.080986
This article has not been copyedited and formatted. The final version may differ from this version.

MATERIALS AND METHODS

Procedures for the synthesis of 7-nitro-5-phenyl-1-(pyrrolidin-1-ylmethyl)-1H-benzo[e][1,4]diazepin-2(3H)-one (neurounina-1)

Formaldehyde (0.1 mL, 3.5 mmol) was added to pyrrolidine (0.3 mL, 3.5 mmol) at 0 °C. The obtained solution was then added to nitrazepam (0.1 g, 0.35 mmol), previously dissolved in glacial acetic acid (5 mL). Next, the reaction mixture was placed in a closed reaction vessel, equipped with temperature control unit, and was irradiated according to the following parameters: initial power, 500 W; initial time, 1 min (ramping); final power, 500 W; T 80 °C; reaction time, 15 min. Afterwards, the reaction mixture was extracted with 2 N NaOH (3 times with 40 mL) and isopropanol/chloroform (1/1, v/v). The organic phase was then washed with brine, dried over anhydrous Na_2SO_4, filtered, and concentrated *in vacuo*. The obtained residue was purified on a silica gel column eluted with dichloromethane/methanol (8/2, v/v) affording 61 mg of purified product (yield 48%) which was converted to the corresponding trifluoroacetate salt by dissolving in 0.1% trifluoroacetic acid (TFA) in H_2O/acetonitrile (60/40, v/v). Finally, the obtained solution was frozen and lyophilized to yield the desired salt.

The final product was analyzed by NMR spectroscopy. In particular, results showed ^{1}H NMR (400 MHz, $CDCl_3$) δ 1.20-1.30 (m, 4H), 1.90-2.10 (m, 4H), 3.20 (s, 2H), 4.20 (s, 2H), 7.33-7.51 (m, 6H), 8.24 (s, 1H), and 8.35 (d, 1H); ESI-MS calcd for $C_{20}H_{20}N_4O_3$364.4 found $[M + H]^+$ 365.1, where ‘s’ was used for singlet, and ‘m’ was used for multiplet. The 1H and 13C NMR spectra were recorded on a Varian Mercury Plus 400 MHz instrument.

Purity of the product was assessed by analytical RP-HPLC using a Beckman C18 column (5 µm, 4.6 x 250 mm) using the following conditions: eluent A, 0.05% TFA (v/v) in water; eluent B, 0.05% TFA (v/v) in acetonitrile; gradient 10-40% B over 25 min, UV detection at

Molecular Pharmacology Fast Forward. Published on October 11, 2012 as DOI: 10.1124/mol.112.080986
This article has not been copyedited and formatted. The final version may differ from this version.

254 nm, flow rate 1 mL/min. The column was connected to a Rheodyne model 7725 injector, a Waters 600 HPLC system, a Waters 486 tunable absorbance detector, and a Waters 746 chart recorder. Neurounina-1 was dissolved in DMSO and diluted in the medium to the final concentrations used. DMSO, at final concentration did not modify both ionic currents and Na^+-dependent Ca^{2+} transport.

Cell Cultures

Baby hamster kidney (BHK) cells stably transfected with canine cardiac NCX1.1, rat brain NCX2.1, and NCX3.3 were a generous gift from Dr. Kenneth D. Philipson (UCLA, Los Angeles, California, USA). All BHK cell lines were grown on plastic dishes in a mix of DMEM and Ham's F12 media (1:1) (Life Technologies, San Giuliano Milanese, Italy) supplemented with 5% fetal bovine serum, 100 U/ml penicillin, and 100 µg/ml streptomycin (Sigma, St. Louis, Missouri, USA). Cells were cultured in a humidified 5% CO_2 atmosphere, and the culture medium was changed every 2 days. For microfluorimetric and electrophysiological studies, cells were seeded on glass coverslips (Fisher, Springfield, NJ) coated with poly-L-lysine (30 µg/ml) (Sigma, St. Louis, MO) and used at least 12h after seeding.

Granule cells were prepared from eight-day-old rats as previously described (Robello et al., 1993), and studied from the 6^{th} to the 10^{th} day *in vitro*.

Generation and Stable Expression of Wild-Type and Mutant Exchangers

All NCX1/NCX3 chimeras shown in Fig. 3 were constructed by Iwamoto's group, as previously thoroughly described (Iwamoto et al., 2004a). Deletion mutant of NCX1, NCX1Δf, was obtained by deleting the amino acid region 241-680 of canine NCX1.1 cDNA with the QuikChange Site-Directed Mutagenesis kit (Stratagene, La Jolla, CA). Substitution

Molecular Pharmacology Fast Forward. Published on October 11, 2012 as DOI: 10.1124/mol.112.080986
This article has not been copyedited and formatted. The final version may differ from this version.

of the amino acid residues in NCX1 was performed by site-directed mutagenesis using the same polymerase chain reaction-based strategy (Stratagene, La Jolla, CA). All mutant exchangers obtained were verified by sequencing both DNA strands (Primm, Milan, Italy).

To stably express chimeric and mutant exchangers, pKCRH or pCEFL plasmids carrying cDNAs were transfected into wild-type BHK cells by Lipofectamine 2000 (Life Technologies, San Giuliano Milanese, Italy) protocol. Cell clones highly expressing Na^+/Ca^{2+} exchange activity were selected by a Ca^{2+}-killing procedure with the Ca^{2+} ionophore ionomycin. In the presence of this ionophore, cells not expressing the exchanger died from Ca^{2+} overload (Iwamoto et al., 1998).

Measurement of Na^+-dependent $^{45}Ca^{2+}$ uptake and $^{45}Ca^{2+}$ efflux

$^{45}Ca^{2+}$ influx into the cells was measured as previously described (Secondo et al., 2007). After treatments, cells cultured in 24-well dishes were incubated in normal Krebs (in mM): 5.5 KCl, 145 NaCl, 1.2 $MgCl_2$, 1.5 $CaCl_2$, 10 glucose, and 10 Hepes-NaOH, pH 7.4 containing 1 mM ouabain and 10 µM monensin at 37°C for 10 min. Then, $^{45}Ca^{2+}$ uptake was initiated by switching the normal Krebs medium to Na^+-free NMDG (in mM): 5.5 KCl, 147 N-Methyl D-glucamine (NMDG), 1.2 $MgCl_2$, 1.5 $CaCl_2$, 10 glucose, and 10 Hepes-NaOH (pH 7.4) containing 10 µM $^{45}Ca^{2+}$ (800 MBq/ml, Perkin Elmer, Italy) and 1 mM ouabain. After 30 seconds incubation, cells were washed with an ice-cold solution containing 2 mM La^{3+} to stop $^{45}Ca^{2+}$ uptake. Cells were subsequently lysed with 0.1 N NaOH and aliquots were taken to determine radioactivity and protein content.

To measure $^{45}Ca^{2+}$ efflux, cells were loaded with 1 µM of $^{45}Ca^{2+}$ (80 MBq/ml) together with 1 µM ionomycin for 60 seconds in normal Krebs. Next, cells were exposed either to a Ca^{2+}- and Na^+-free solution —a condition that blocks both intracellular $^{45}Ca^{2+}$ efflux and extracellular Ca^{2+} influx— or to a Ca^{2+}-free plus 2 mM EGTA containing 145 mM Na^+ —a

Molecular Pharmacology Fast Forward. Published on October 11, 2012 as DOI: 10.1124/mol.112.080986
This article has not been copyedited and formatted. The final version may differ from this version.

condition that promotes $^{45}Ca^{2+}$ efflux. One µM thapsigargin was present in both solutions. $^{45}Ca^{2+}$ efflux was started by using Ca^{2+}-free-Na^{+} containing solution plus 2 mM EGTA. Cells were exposed to this solution, which promotes $^{45}Ca^{2+}$ efflux, for 10 seconds. At the time chosen (10 seconds), a very low efflux was detected in wild-type BHK cells. Na^{+}_{0}-dependent $^{45}Ca^{2+}$ efflux was estimated by subtracting $^{45}Ca^{2+}$ efflux in Ca^{2+}- and Na^{+}-free solution from that in Ca^{2+}-free solution. Cells were subsequently lysed with 0.1 N NaOH, and aliquots were taken to determine radioactivity and protein content by Bradford method. The EC_{50}s of neurounina-1 were obtained by fitting the data with the equation: a + b • exp(-x/t), where "*a*" is the maximal response, "b" is the basal response, "*x*" is the drug concentration, and "*t*" is the EC_{50}.

$[Ca^{2+}]_i$ Measurement

$[Ca^{2+}]_i$ was measured by single cell computer-assisted video imaging (Secondo et al., 2007). Briefly, BHK cells, grown on glass coverslips, were loaded with 6 µM Fura-2 acetoxymethyl ester (Fura-2AM) for 30 minutes at 37°C in normal Krebs solution containing the following (in mM): 5.5 KCl, 160 NaCl, 1.2 $MgCl_2$, 1.5 $CaCl_2$, 10 glucose, and 10 Hepes-NaOH, pH 7.4. At the end of the Fura-2AM loading period, the coverslips were placed into a perfusion chamber (Medical System, Co. Greenvale, NY, USA) mounted onto the stage of an inverted Zeiss Axiovert 200 microscope (Carl Zeiss, Germany) equipped with a FLUAR 40X oil objective lens. The experiments were carried out with a digital imaging system composed of MicroMax 512BFT cooled CCD camera (Princeton Instruments, Trenton, NJ, USA), LAMBDA 10-2 filter wheeler (Sutter Instruments, Novato, CA, USA), and Meta-Morph/MetaFluor Imaging System software (Universal Imaging, West Chester, PA, USA). After loading, cells were alternatively illuminated at wavelengths of 340 nm and 380 nm by a Xenon lamp. The emitted light was passed through a 512 nm

Molecular Pharmacology Fast Forward. Published on October 11, 2012 as DOI: 10.1124/mol.112.080986
This article has not been copyedited and formatted. The final version may differ from this version.

barrier filter. Fura-2 fluorescence intensity was measured every 3 seconds. Forty to sixty-five individual cells were selected and monitored simultaneously from each cover slip. All the results are presented as cytosolic Ca^{2+} concentration. Since K_D for Fura-2 was assumed to be 224 nM, the equation of Grynkiewicz (Grynkiewicz et al., 1985) was used for calibration. NCX activity was evaluated as Ca^{2+} uptake through the reverse mode by switching the normal Krebs medium to Na^+-deficient $NMDG^+$ medium named Na^+-free (in mM: 5.5 KCl, 147 N-Methyl glucamine, 1.2 $MgCl_2$, 1.5 $CaCl_2$, 10 glucose, and 10 Hepes-Trizma, pH 7.4) in the presence of thapsigargin, the irreversible and selective inhibitor of the sarco(endo)plasmic reticulum Ca^{2+} ATPase (SERCA) (Secondo et al., 2007).

Neurounina-1 was incubated with cells for 30 minutes before NCX activity was studied. Each EC_{50} of neurounina-1 was obtained fitting the data with the equation: $a + b \bullet \exp(-x/t)$, where “a” is the maximal response, “b” is the basal response, “x” is the drug concentration, and “t” is the EC_{50}.

The activity of the NMDA receptor was studied as $[Ca^{2+}]_i$ increase detected in cortical neurons (10 DIV) when rapidly exposed to NMDA (100 µM) and glycine (10 µM) in a Mg^{2+}-free solution.

Electrophysiology

NCX currents

NCX currents (I_{NCX}) were recorded, by patch-clamp technique in whole-cell configuration (Molinaro et al., 2008; Molinaro et al., 2011; Secondo et al., 2007), in the following groups: (a) wild-type BHK, (b) BHK stably transfected with NCX1, (c) NCX2 and (d) NCX3. Each experimental group was exposed to neurounina-1 or its vehicle. Currents were filtered at 5 kHz and digitized using a Digidata 1322A interface (Molecular Devices). Data were acquired and analyzed using the pClamp software (version 9.0, Molecular Devices).

Molecular Pharmacology Fast Forward. Published on October 11, 2012 as DOI: 10.1124/mol.112.080986
This article has not been copyedited and formatted. The final version may differ from this version.

Briefly, I_{NCX} was recorded starting from a holding potential of -70 mV up to a short-step depolarization at +60 mV (60 ms) (Secondo et al., 2009). Then, a descending voltage ramp from +60 mV to -120 mV was applied. The current recorded in the descending portion of the ramp (from +60 mV to -120 mV) was used to plot the current-voltage (I-V) relation curve. The magnitudes of I_{NCX} were measured at the end of +60 mV (reverse mode) and at the end of -120 mV (forward mode), respectively. In order to isolate I_{NCX}, the same cells of all experimental groups were firstly recorded for total currents, and then for the currents in presence of Ni^{2+} (5 mM), a selective blocker of I_{NCX}. To obtain the isolated I_{NCX}, the Ni^{2+}-insensitive unspecific currents were subtracted from the total currents ($I_{NCX}=I_T - I_{NiResistant}$) (Molinaro et al., 2008; Molinaro et al., 2011; Secondo et al., 2011). In all experimental groups, both neurounina-1-treated and non-treated cells were recorded before and after $NiCl_2$ exposure. Neurounina-1-induced I_{NCX} increase was calculated as follows: ($I_{NCXneurounina\text{-}1}/I_{NCXcontrol}$)x100. External Ringer solution contained (in mM): NaCl 126, $NaHPO_4$ 1.2, KCl 2.4, $CaCl_2$ 2.4, $MgCl_2$ 1.2, glucose 10 and $NaHCO_3$ 18, TEA 20, TTX 10 nM, and nimodipine 10 μM (pH 7.4). The dialysing pipette solution contained (mM): K-gluconate 100, tetraethylammonium (TEA) 10, NaCl 20, Mg-ATP 1, and 0.1 $CaCl_2$, 2 $MgCl_2$, 0.75 EGTA, Hepes 10, adjusted to pH 7.2 with CsOH. TEA (20 mM) and Cs were included to block delayed outward rectifier K^+ components; nimodipine (10 μM) and TTX (50 nM) were added to external solution to block L-type Ca^{2+}-channels and TTX-sensitive Na^+-channels, respectively. The quantifications of I_{NCX} were normalized for membrane capacitance and expressed as percentage of controls as previously reported (Molinaro et al., 2008; Molinaro et al., 2011), whereas the representative traces of I_{NCX} are expressed as pA/mV. The reversibility of neurounina-1 effect on I_{NCX} was measured in the same BHK-NCX1 or BHK-NCX2 cells exposing them to 10 nM neurounina-1 and after 5 minutes of drug washout.

Molecular Pharmacology Fast Forward. Published on October 11, 2012 as DOI: 10.1124/mol.112.080986
This article has not been copyedited and formatted. The final version may differ from this version.

To obtain the EC_{50} of neurounina-1 on each aforementioned current, all data were fitted to the following binding isotherm: $y = max / (1 + (X/EC_{50}))^n$, where '*X*' is the drug concentration and '*n*' is the Hill coefficient.

$GABA_A$ currents

In these experiments, membrane currents were measured with the standard whole-cell patch-clamp technique using an Axopatch 200B amplifier (Axon Instruments) on rat cerebellar granule cells. Patch pipettes were prepared from borosilicate glass capillaries (Type 1304336 TW 150-3 World Precision Instruments Florida, USA) with the model P-30 puller (Sutter Instruments Co., USA). In all the experiments reported, the holding potential was set at -80 mV, since it resulted as the most suitable condition for recording the total chloride current elicited by GABA. Ionic currents were recorded with a Labmaster D/A, A/D converter driven by pClamp software (Axon Instruments, Burlingame, CA, USA). Analysis was performed with pClamp 7 and SigmaPlot software 9.0 (Jandel Scientific, Ekrath, Germany). The standard external solution contained (in mM): 135 NaCl, 5.4 KCl, 1.8 $CaCl_2$, 1 $MgCl_2$, 5 Hepes, and 10 glucose; pH 7.4 was adjusted with NaOH. The internal solution contained (in mM): 142 KCl, 10 Hepes, 2 EGTA, 1 $MgCl_2$, and 3 ATP; pH was adjusted to 7.3 with Tris base. GABA and neurounina-1 were diluted with the external solution at the desired final concentration just before experiments were performed. The external solution was applied to the cell bath by steady perfusion (around 3 ml/min gravity flow). In all the experiments, the peak chloride current evoked by GABA in the presence of neurounina-1 was referred to those activated by plain GABA in the same cell. In particular, neurounina-1-induced current increase was expressed as $E\%=100 \times (I_{N+GABA} - I_{GABA})/ I_{GABA,}$ where I_{N+GABA} represents the current in the presence of neurounina-1 plus GABA, whereas I_{GABA} represents the current with GABA alone. The concentration-response curves for the

Molecular Pharmacology Fast Forward. Published on October 11, 2012 as DOI: 10.1124/mol.112.080986
This article has not been copyedited and formatted. The final version may differ from this version.

compound can be fitted by Hill equation: $E\%=E\%_{max}\ C^n / C^n + K^n$ where $E\%_{max}$ is the maximal percentage of enhancement, *C* is the drug concentration, *n* is the Hill number, and *K* is the concentration, where $E\% = E\%_{max}/2$.

***In vitro* Toxicity**

BHK-NCX1, BHK-NCX2, and BHK-NCX3 cell lines were exposed to 10 μM neurounina-1 at 37 °C in a humidified 5% CO_2 atmosphere. After 24h of incubation, cell injury was assessed using a mixture of the fluorescent dyes propidium iodide (PI) and fluorescein diacetate (FDA) (Life Technologies) at the final concentrations of 7 μM and 36 μM, respectively. PI- and FDA-positive cells were counted in three representative fields of independent cultures obtained with a 40X objective, and cell death was determined by the ratio of the number of PI-positive cells/PI+FDA positive cells (Secondo et al., 2007).

Determination of Mitochondrial Activity

Mitochondrial dysfunction was evaluated with the MTT method (Secondo et al., 2007). In brief, after the experimental procedures, BHK-NCX1, BHK-NCX2, and BHK-NCX3 cells were washed with normal Krebs solution and incubated with 1 ml of MTT solution (0.5 mg/ml in phosphate-buffered saline). This yellow water-soluble tetrazolium salt is converted into a water-insoluble purple formazan by the succinate dehydrogenase system of the active mitochondria. Therefore, the amount of formazan produced is proportional to the number of cells with mitochondria that are still alive. After 1h of incubation at 37 °C, cells were dissolved in 1 ml of DMSO, in which the rate of MTT reduction was measured by a spectrophotometer at a wavelength of 540 nm. Data are expressed as percentage of mitochondrial dysfunction versus sham-treated cultures.

Molecular Pharmacology Fast Forward. Published on October 11, 2012 as DOI: 10.1124/mol.112.080986
This article has not been copyedited and formatted. The final version may differ from this version.

In vitro model of ischemia

Cortical neurons were prepared from brains of Wistar rat pups 2–4 days postpartum. The tissue was minced and trypsinized (0.1% for 15 min at 37°C), triturated, and plated on poly-D-lysine-coated coverslips and cultured in Neurobasal medium (Invitrogen) supplemented with B-27 (Invitrogen) and 2mM L-glutamine. Cells were plated at concentration of $1.8x10^6$ on 25-mm glass coverslips. Cultures were maintained at 37°C in a humidified atmosphere of 5%CO2 and 95% air, fed twice a week, and maintained for a minimum of 10 days before experimental use (Scorziello et al., 2007).

Hypoxic conditions were induced by exposing cortical neurons to oxygen- and glucose free-medium in a humidified atmosphere containing 95% nitrogen and 5% CO_2 (Scorziello et al., 2007). After 3h of OGD, reoxygenation was induced by exposing cortical neurons to the previous MEM/F12 medium containing glucose and oxygen. After 21h of reoxygenation, cell injury was assessed using the fluorescent dyes PI (7 μM) and FDA (36 μM) (Life Technologies). PI- and FDA-positive cells were counted in three representative fields of independent cultures, and cell death was determined by the ratio of the number of PI-positive cells/PI+FDA positive cells.

Experimental Animal Groups

Wild-type male C57/BL6 mice (Charles River, Italy) aged between 6-8 weeks and weighing 27-30 g were housed under diurnal lighting conditions. Each experimental group included at least 5 animals. Experiments were performed according to the international guidelines for animal research and approved by the Animal Care Committee of “Federico II”, University of Naples, Italy.

Transient Middle-Cerebral Artery Occlusion Model (tMCAo)

Molecular Pharmacology Fast Forward. Published on October 11, 2012 as DOI: 10.1124/mol.112.080986
This article has not been copyedited and formatted. The final version may differ from this version.

Mice were anesthetized using a mixture of 5% sevoflurane in a 70% nitrous oxide/30% oxygen and anaesthesia was maintained during the surgical procedure with 2% sevoflurane. Transient MCAo was induced as previously described (Cuomo et al., 2008; Molinaro et al., 2008). Briefly, a 5-0 nylon filament was inserted through the external carotid artery stump and advanced into the left internal carotid artery until it blocked the origin of the middle cerebral artery (MCA). After 60-min MCA occlusion, the filament was withdrawn to restore blood flow. Body temperature was monitored throughout the entire duration of the surgical procedure and maintained at 37.5 °C with a thermostatic blanket.

Monitoring of blood gas concentration and cerebral blood flow (CBF) with laser-doppler flowmetry

A catheter was inserted into the femoral artery to measure arterial blood gases before and after ischemia (Rapid lab 860; Chiron Diagnostic). CBF was monitored in the cerebral cortex ipsilateral to the occluded MCA with a laser-doppler flowmeter (Periflux system, 5000) (Cuomo et al., 2007). Once a stable CBF signal was obtained, the MCA was occluded. CBF monitoring was continued up to 30 minutes after the end of the surgical procedure once the occurred reperfusion was verified. Only the animals showing a reduction in CBF of at least 70% were included in the experimental groups and no difference in reduction in CBF was present among the experimental groups. The percentage of CBF reduction in the different experimental groups was: (a) 77.1±1.07% in vehicle treated group; (b) 77.5±0.5% in 3 ng/kg neurounina-1 3 hours after ischemia; (c) 77.8±0.93% in 10 ng/kg neurounina-1 3 hours after ischemia; (d) 76.3±0.9% in 30 ng/kg neurounina-1 3 hours after ischemia; (e) 77.3±0.6% in 3 μg/kg neurounina-1 3 hours after ischemia; (f) 77.5±0.5% in 30 μg/kg neurounina-1 3 hours after ischemia; (g) 76.8±0.6% in

Molecular Pharmacology Fast Forward. Published on October 11, 2012 as DOI: 10.1124/mol.112.080986
This article has not been copyedited and formatted. The final version may differ from this version.

30 ng/kg neurounina-1 5 hours after ischemia; (h) 76.7±1.45% in 3 μg/kg neurounina-1 5 hours after ischemia; (i) 77.3±0.6% in 30 μg/kg neurounina-1 5 hours after ischemia; (j) 76.8±0.6% in 10 mg/kg flumazenil; (k) 77.8±0.7% in 30 ng/kg neurounina-1 + 10 mg/kg flumazenil.

Evaluation of ischemic volume

The ischemic area was evaluated by 2,3,5-triphenyltetrazolium chloride (TTC) staining (Pignataro et al., 2004a). Briefly, mice were decapitated 24 h after tMCAO. The brains were quickly removed and placed in ice-cold saline for 5 minutes and then cut into 500 μM coronal slices with a vibratome (Campden Instrument, 752M; UK). Sections were incubated in 2% TTC containing saline solution for 20 minutes and in 10% formalin overnight. The infarcted area was calculated by image analysis software (Image-Pro Plus) (Pignataro et al., 2004a). Total infarct volume was expressed as percentage of the volume of the hemisphere ipsilateral to the lesion in order to eliminate the effect of brain swelling on the total calculated infarct volume (Pignataro et al., 2004a).

Experimental protocol for drug administration

Neurounina-1 saline solution was administered intraperitoneally at the doses of 0.003, 0.01, 0.03, 3, and 30 μg/kg 3h after tMCAO, or at the doses of 0.03, 3 and 30 μg/kg 5h after ischemia induction. Flumazenil was administered intraperitoneally at the dose of 10 mg/kg three times, 3h, 4h, and 5h after tMCAO. All experiments were carried out in blind manner, the person who performed the experiments and analyse the data was not aware of the pharmacological treatment. The body temperature of mice were monitored every hour starting from 1 hour after neurounina-1 administration until 6 hours. Vehicle-treated

Molecular Pharmacology Fast Forward. Published on October 11, 2012 as DOI: 10.1124/mol.112.080986
This article has not been copyedited and formatted. The final version may differ from this version.

group displayed 36.93±0.03 °C, whereas 0.03 μg/kg neurounina-1-treated group displayed 36.87±0.04 °C.

Synaptosomes purification

Rats were sacrificed, the brains were rapidly removed and the cerebral cortex dissected at 4°C. Synaptosomes were prepared essentially as previously described (Stigliani et al., 2006). The tissue was homogenized in 10 volumes (1 g in 10 mL) of 0.32M sucrose, buffered at pH 7.4 with Tris-HCl, using a glass-teflon tissue grinder (clearance 0.25 mm). The homogenate was centrifuged (5 min, 1,000 x g) to remove nuclei and debris and the supernatant was gently stratified on a discontinuous Percoll® gradient (2, 6, 10 and 20% v/v in Tris-buffered sucrose). After centrifugation at 33,500 x g for 5 min, the layer between 10 and 20% Percoll® (synaptosomal fraction) was collected, washed by centrifugation at 20,000 x g for 15 min and then resuspended in physiological medium having the following composition (mM): NaCl, 140; KCl, 3; $MgSO_4$ 1.2; NaH_2PO_4, 1.2; $NaHCO_3$ 5; $CaCl_2$ 1.2; HEPES 10; glucose, 10; pH 7.4. Proteins were measured according to Bradford method using bovine serum albumin as a standard. All the above procedures were performed at 4°C.

Release experiments

Synaptosomes were incubated at 37°C for 15 min; aliquots of synaptosomal suspension (about 300 μg protein) were equally layered on microporous filters placed at the bottom of a set of parallel superfusion chambers maintained at 37°C (Superfusion System, Ugo Basile, Comerio, Varese, Italy; (Tardito et al., 2010)). Superfusion was then started with standard medium at a rate of 0.5 ml/min and continued for 48 min. After 36 min of superfusion to equilibrate the system, samples were collected according to the

Molecular Pharmacology Fast Forward. Published on October 11, 2012 as DOI: 10.1124/mol.112.080986
This article has not been copyedited and formatted. The final version may differ from this version.

following scheme: two 3-min samples (t= 36–39 min and t =45–48 min; basal outflow) before and after one 6-min sample (t= 39–45 min; stimulus-evoked release). A 90-sec period of stimulation was applied at t= 39 min, after the collection of the first sample.

Stimulation of synaptosomes was performed with 15 mM KCl, substituting for equimolar concentration of NaCl. In the first experimental group, in which the calcium dependence was assessed, a Ca^{2+}-free medium was added at 20 min and maintained during the KCl pulse period; in the second and third groups, in which the carrier mediate component of glutamate or GABA release was evaluated, the broad spectrum glutamate uptake inhibitor DL-TBOA (10 µM) or the selective GAT1 transporters inhibitor SKF89976A (10 µM) were respectively added at 30 min and maintained during the KCl pulse period; in the fourth group, in which the effect of neurounina-1 (10-30-100 nM) was measured on neurotransmitter release, the drug was added at 30 min and maintained during the 15 mM KCl stimulation pulse period.

Collected samples were analysed for endogenous glutamate and GABA content. Amino acid release was expressed as pmol/mg of protein. The stimulus-evoked overflow was estimated by subtracting the transmitter content of the two 3-min samples (basal outflow) from the release evoked in the 6-min sample collected during and after the depolarization pulse (stimulus-evoked release).

Neurotransmitter release determination

Endogenous glutamate and GABA content was measured by high performance liquid chromatography analysis following pre-column derivatization with o-phthalaldehyde and gradient separation on a C18 reverse-phase chromato-graphic column (10 x 4.6 mm, 3 µm; at 30°C; Chrompack, Middleburg, The Netherlands) coupled with fluorometric

Molecular Pharmacology Fast Forward. Published on October 11, 2012 as DOI: 10.1124/mol.112.080986
This article has not been copyedited and formatted. The final version may differ from this version.

detection (excitation wavelength 350 nm; emission wavelength 450 nm). Homoserine was used as an internal standard. For more details, see Tardito et al. (2010).

Statistical analysis

Data are expressed as mean (± SEM) of six independent determinations. LogP value of neurounina-1 was calculated on the basis of ChemDraw 11.0 software. Statistical comparisons between controls and treated experimental groups were performed using the one-way ANOVA, followed by Newman Keul's test. $p < 0.05$ was considered statistically significant.

Molecular Pharmacology Fast Forward. Published on October 11, 2012 as DOI: 10.1124/mol.112.080986
This article has not been copyedited and formatted. The final version may differ from this version.

RESULTS

Neurounina-1 increases NCX1 and NCX2 activity in stably transfected BHK cells, as revealed by Ca^{2+} radiotracer influx/efflux and Fura-2 microfluorimetry techniques

The newly synthesized compound neurounina-1, whose structure is illustrated in the inset of Fig 1A, increased NCX1 and NCX2 activity in a concentration-dependent manner. Remarkably, it displayed a high potency with an EC_{50} in the low nanomolar range (1.1 – 2.7 nM) and in the picomolar range (34 – 87 pM), as detected by Ca^{2+} radiotracer and Fura-2 monitored Ca^{2+} influx techniques, respectively. Furthermore, these changes occurred in both forward and reverse modes of operation, as revealed by Na^+-dependent $^{45}Ca^{2+}$ influx/efflux methods (Fig 1A and B) and by Na^+-free-induced $[Ca^{2+}]_i$ increases in single cells (Fig 1C). By contrast, neurounina-1 was substantially ineffective on NCX3-mediated influx and efflux at concentrations even up to 10 μM (Fig 1A and B).

Neurounina-1 increases NCX1 and NCX2 activity in stably transfected BHK cells, as revealed by patch-clamp technique

In stably transfected BHK cells, 10 nM neurounina-1 significantly increased NCX1 and NCX2 currents, recorded by patch-clamp technique, in both forward and reverse modes of operation (Fig 2A and B). In particular, NCX1 activity was increased by ~60% and that of NCX2 by ~40%. By contrast, neurounina-1 did not affect I_{NCX} in BHK-NCX3 as well as unspecific currents in BHK wild-type cell lines (Fig 2C and D). Five minutes of wash-out completely reverted neurounina-1-induced increase in both NCX1 and NCX2 activities (Fig 2A and B).

Molecular Pharmacology Fast Forward. Published on October 11, 2012 as DOI: 10.1124/mol.112.080986
This article has not been copyedited and formatted. The final version may differ from this version.

α_1 and α_2 repeats are the molecular determinants of the neurounina-1 stimulatory effect on NCX1

To investigate the molecular determinants of neurounina-1 responsible for NCX1-stimulatory activity, the intracellular f-loop, a region mainly involved in the regulation of NCX function, was deleted. In particular, despite the f-loop deletion, 10 nM neurounina-1 was still able to increase the activity of the mutant NCX1Δ241–680 (NCX1Δf) in both forward and reverse modes of operation (Fig 3A and B), suggesting that the f-loop is not a critical region for neurounina-1 binding and activity. Taking advantage of the fact that NCX1 was sensitive to neurounina-1, whereas NCX3 was insensitive despite the high sequence homology between the two isoforms, we carried out experiments with chimeras obtained between these two NCX isoforms in order to identify the region(s) responsible for the stimulatory effect of neurounina-1 in the NCX1 molecule. In particular, we used a series of chimeras in which a segment from NCX3.3 was transferred into NCX1.1 in exchange for the homologous segment(s) (Iwamoto et al., 2004b) and *vice versa* (Fig 3). All chimeras used exhibited basal exchange activities similar to that of the wild-type NCX1 (Iwamoto et al., 2004b). Figure 3 shows the effects of 10 nM neurounina-1 on the rates of Na^+-dependent $^{45}Ca^{2+}$ efflux/influx into BHK cells expressing wild-type or chimeric exchangers. Ten nanomolar of neurounina-1 increased the $^{45}Ca^{2+}$ efflux/influx rates of the wild-type NCX1 to approximately 70% and 35% of the respective controls. $NCX1_{193/445}$ chimera, containing the fifth transmembrane domain and the N-terminal portion of the cytosolic f loop of NCX3, showed a significant increased activity in the presence of 10 nM neurounina-1, in both forward and reverse modes of operation. A similar increase was observed in $NCX1_{718/787}$ chimera, containing the C-terminal portion of the cytosolic f loop and the sixth transmembrane domain of NCX3 (Fig 3A and B).

Molecular Pharmacology Fast Forward. Published on October 11, 2012 as DOI: 10.1124/mol.112.080986
This article has not been copyedited and formatted. The final version may differ from this version.

By contrast, $NCX1_{109/133}$ chimera, which contained the α_1 repeat of NCX3, and $NCX1_{788/829}$ chimera, which contained the α_2 repeat of NCX3, displayed no significant increased activity in the presence of 10 nM neurounina-1 in both modes of operation (Fig 3A and B), thereby indicating that these two segments are necessary for drug activity.

Interestingly, a chimera of the neurounina-1-insensitive NCX3 isoform, in which the α_1 and α_2 regions were substituted with the corresponding sequences of the neurounina-1-sensitive NCX1 isoform, became responsive to the drug (Fig. 3A and 3B). This finding further indicates that the α_1 and α_2 segments are exclusively responsible for the different drug responses between NCX1 and NCX3.

Val118, Asn125, and Leu808 are responsible for NCX1 sensitivity to neurounina-1

To establish the sites responsible for the stimulatory action of neurounina-1 on NCX1 activity, we substituted individual critical residues of the α_1 and α_2 regions of NCX1.1 with the corresponding amino acid present on the neurounina-1-insensitive NCX3 isoform (Fig 4A). Each NCX1 mutant was singly and stably transfected in wild-type BHK cells. In NCX1V118L, NCX1N125G (α_1 repeat), and NCX1L808F (α_2 repeat) mutants, neurounina-1 was unable to elicit an increase in the antiporter activity, as revealed by the Ca^{2+} radiotracer (Fig. 4B) and single-cell Fura-2-monitored Ca^{2+} microfluorimetry techniques (Fig 4C). These data suggest that these three residues are critical for NCX1 sensitivity to the drug. In addition, in two of the three mutants, *i.e.*, NCXV118L and NCX1N125G, the stimulatory effect of neurounina-1 was converted into an inhibitory effect. Since the inhibition of NCX1 by several drugs such as KB-R7943, SEA0400, SN-6, and YM-244769 depends on Gly833 (Iwamoto et al., 2004a; Iwamoto et al., 2004b; Iwamoto et al., 2001), we tested whether neurounina-1 was still active on the mutant NCX1G833C lacking this

Molecular Pharmacology Fast Forward. Published on October 11, 2012 as DOI: 10.1124/mol.112.080986
This article has not been copyedited and formatted. The final version may differ from this version.

apolar amino acid. Interestingly, the substitution of the critical residue Gly833 with cysteine on NCX1 did not prevent the stimulatory effect of neurounina-1 (Fig. 4B and 4C).

Neurounina-1 does not induce cell death and mitochondrial dysfunction in stably transfected BHK-NCX1, BHK-NCX2, and BHK-NCX3 cells

The toxicity of neurounina-1 was evaluated *in vitro* by exposing BHK-NCX1, BHK-NCX2 and BHK-NCX3 cells to 10 μM neurounina-1, a concentration 10^4 times higher than the calculated EC_{50}s. Neurounina-1 incubation for 24h did not cause any cell death measured by PI/FDA+PI method (Fig 5A) or any significant decrease in mitochondrial activity as revealed by MTT method (Fig. 5B).

Neurounina-1 reduces cell death in primary cortical neurons exposed to oxygen and glucose deprivation plus reoxygenation

Primary cortical neurons exposed to 3h of oxygen and glucose deprivation (OGD) followed by 21h of reoxygenation were used to investigate the neuroprotective effects of neurounina-1 in an *in vitro* model of anoxia. Ten nanomolar of neurounina-1 exerted a remarkable neuroprotective effect by reducing cell death induced by OGD and OGD plus reoxygenation (Fig 5C).

Neurounina-1 reduces ischemic brain damage in mice subjected to tMCAO

Remarkably, prediction analysis revealed that neurounina-1 possesses a high lipophilicity and, thus, a high capability of crossing the blood brain barrier with an estimated logP of 0.87 (n-ottanol/water).

Consistent with *in vitro* results, the intraperitoneal injection of neurounina-1 in a single dose ranging from 0 to 30 μg/kg in C57B male mice, previously subjected to 60 minutes of

Molecular Pharmacology Fast Forward. Published on October 11, 2012 as DOI: 10.1124/mol.112.080986
This article has not been copyedited and formatted. The final version may differ from this version.

middle cerebral artery occlusion (MCAO) followed by 23h of reperfusion, caused a dose-dependent reduction in the ischemic volume compared to vehicle-treated mice (Fig 6A and B), even when administered in the low nanograms/kg range. In particular, 3 ng/kg neurounina-1, administered 3h after stroke onset, produced a mild, but nonetheless significant decrease (~20%) of the ischemic damage. Higher doses of neurounina-1 from 30 ng/kg up to 30 μg/kg produced a more remarkable neuroprotective effect, causing a 60% reduction of the ischemic brain damage. More important, at the dose of 30 μg/kg, neurounina-1 displayed a wide therapeutic window as it was still effective even 5h after stroke induction (Fig 6B). The mortality rate in all neurounina-1-treated groups was around 5% as observed for the control groups.

Neurounina-1 increases the $GABA_A$-mediated currents of chloride ions

Since neurounina-1 contains a benzodiazepine-like structure, we tested whether it could increase the $GABA_A$-mediated currents. Neurounina-1 at 10 nM did not affect the chloride currents *per se* (data not shown); however in the presence of 10 μM GABA, neurounina-1 increased the peak of chloride current in a concentration-dependent manner with an EC_{50} of 3.6 nM. The neurounina-1 effect on $GABA_A$ currents was reverted by 10 μM flumazenil (Fig 7A and B). The maximum increase of the $GABA_A$ currents was observed at neurounina-1 concentrations higher than 10 nM (Fig 7C).

The benzodiazepine antagonist, flumazenil, does not revert the neuroprotective effect of neurounina-1 in mice subjected to tMCAO

To verify whether the effect of neurounina-1 during cerebral ischemia was mediated by the activation of $GABA_A$ receptors, we evaluated the effect of this compound on the ischemic

Molecular Pharmacology Fast Forward. Published on October 11, 2012 as DOI: 10.1124/mol.112.080986
This article has not been copyedited and formatted. The final version may differ from this version.

brain damage in the presence of the benzodiazepine-antagonist flumazenil. Mice were treated with three injections of 10 mg/kg flumazenil (Brogden and Goa, 1988) at 3, 4, and 5h after ischemia induction and with neurounina-1, at the dose of 0.03 μg/kg, 3h after ischemia induction. Under these conditions, flumazenil did not revert the neuroprotection induced *in vivo* by neurounina-1 after transient MCAO and flumazenil alone did not influence the extent of the infarct volume as compared to vehicle-treated ischemic mice (Fig. 7D).

Neurounina-1 inhibits 15 mM KCl-evoked endogenous glutamate and GABA releases in synaptosomes and NMDA receptor activation.

Since neurounina-1 has a neuroprotective effect on an *in vitro* model of cerebral ischemia, we tested whether it could interfere with glutamate/GABA release and/or NMDA receptor activation. Ten micromolar DL-TBOA, a broad spectrum glutamate uptake inhibitor, and 10 μM SKF89976A, a selective GAT1 transporter inhibitor, did not interfere with KCl-evoked glutamate and GABA release, respectively.

Neurounina-1, at concentrations ranging from 10 to 100 nM, did not affect basal release of endogenous glutamate and GABA neurotransmitters (Table 1), but decreased only 15 mM KCl-evoked endogenous glutamate and GABA release from rat brain cortical synaptosomes (Fig 8). On the other hand, 10 nM neurounina-1 inhibited NMDA-induced $[Ca^{2+}]_i$ increase of ~50% (Fig. 8C), whereas the NMDA receptor blocker, MK-801, totally prevented Ca^{2+} influx induced by NMDA perfusion.

Molecular Pharmacology Fast Forward. Published on October 11, 2012 as DOI: 10.1124/mol.112.080986
This article has not been copyedited and formatted. The final version may differ from this version.

DISCUSSION

The present study demonstrated that neurounina-1, a compound synthesized in our laboratories and obtained by modifying the structure of the powerful NCX1 inhibitor, SM-15811 (Hasegawa et al.,2003), is the first molecule that enhances NCX1 and NCX2 activity and also exerts a remarkable neuroprotective effect in stroke.

Interestingly, neurounina-1 displayed a potent and reversible stimulatory effect on NCX1 and NCX2 in both forward and reverse modes of operation, with an estimated EC_{50} in the low-nanomolar range. By contrast, this compound did not affect the activity of NCX3 isoform in the range of 0.001–10μM. These pharmacodynamic properties were confirmed by using three different methods to evaluate NCX function: Ca^{2+} radiotracer influx/efflux, Fura-2 microfluorimetry, and patch-clamp electrophysiology in whole-cell configuration. To characterize the molecular determinants responsible for neurounina-1 activity on NCX1, we used chimera strategy, deletion and site-directed mutagenesis. The removal of the NCX1 f-loop (aa 241-680), a region involved in NCX activity regulation, did not prevent the stimulatory effect of neurounina-1, suggesting that this region is not involved in the binding and stimulatory activity of the drug on NCX1. By contrast, the use of NCX1/NCX3 chimeras allowed us to identify the two amino-acid sequences required for the biochemical interaction between NCX1 and neurounina-1, *i.e*, 109-133 and 788-829, the former corresponding to the α_1-repeat and the latter to the α_2-repeat. Site-directed mutagenesis, instead, allowed us to identify the molecular determinants for neurounina-1 pharmacological action on NCX1. In particular, the three amino-acids, Val118 and Asn125, present in the α_1-repeat, and Leu808, present in the α_2-repeat, were essential to elicit the effect of the drug on the exchanger. Interestingly, these three amino-acids, which

Molecular Pharmacology Fast Forward. Published on October 11, 2012 as DOI: 10.1124/mol.112.080986
This article has not been copyedited and formatted. The final version may differ from this version.

specifically determined NCX1.1 sensitivity to this new compound, were also present in all NCX1 splice variants, including the neuronal forms NCX1.4, NCX1.5, NCX1.12, and in the corresponding sites of the only known splice variant of NCX2, NCX2.1. The relevance of α_1 and α_2 regions in determining NCX1 and NCX2 sensitivity to neurounina-1 is further supported by evidence that the neurounina-1-insensitive NCX3 isoform became sensitive when its α_1 and α_2 regions were substituted with the corresponding regions of NCX1. Noticeably, the substitution of Gly833, a common molecular determinant for several NCX1 inhibitors, with cysteine did not prevent the stimulatory effect of neurounina-1, thus suggesting that the sites of action of some NCX inhibitors may differ from those of neurounina-1. Another peculiar aspect that needs to be underlined is the high potency of neurounina-1 on NCX1 and NCX2 in both forward and reverse modes. In fact, most of drugs that inhibit NCX, including KB-R7943, YM-244769 and SN-6, display an activity in the micromolar range, whereas neurounina-1 exerts its effect on NCX1 and NCX2 in picomolar and low-nanomolar range of concentrations with an EC_{50} of 1-0.1nM. Moreover, at variance with most of NCX inhibitors (Annunziato et al.,2004;Iwamoto and Kita,2006; Iwamoto et al.,1996), neurounina-1 did not display a significant difference between the potency in the forward and reverse mode of operation. Finally, it should be mentioned that neurounina-1 similarly to NCX inhibitors displayed a reversibility of the stimulatory effect as demonstrated by patch-clamp evaluation.

Since the specific knocking-down or knocking-out of the three NCX isoforms worsens ischemic brain damage in *in vitro* and in *in vivo* models of cerebral ischemia (Jeon et al.,2008;Molinaro et al.,2008;Pignataro et al.,2004a) it was conceivable to hypothesize that the activation of this exchanger could be neuroprotective in stroke. Indeed, the stimulation of the antiporter, by modifying the dysregulation of intracellular Na^+ and Ca^{2+} ion homeostasis, could help the rescue of injured neurons in the ischemic and peri-ischemic

Molecular Pharmacology Fast Forward. Published on October 11, 2012 as DOI: 10.1124/mol.112.080986
This article has not been copyedited and formatted. The final version may differ from this version.

areas of the brain. However, to date, only non-selective NCX activators are available such as lithium (Iwamoto et al.,1999), redox agents (Reeves et al.,1986;Secondo et al.,2011), agonists of G-protein–coupled receptors (Annunziato et al.,2004;Eriksson et al.,2001; Stengl et al.,1998;Woo and Morad,2001), diethylpyrocarbonate (Ottolia et al.,2002), concavallin A, NGF, and insulin (Formisano et al.,2008;Gupta et al.,1986;Makino et al.,1988) have been reported to stimulate NCX activity. However, all of these compounds do not possess the pharmacological properties necessary to become valid active drug. Neurounina-1 does instead display some interesting pharmacological properties for a number of reasons. First, its lipophilicity index, determined by logP prediction, is indicative of having a good blood brain barrier permeability. Second, being water soluble, it is injectable by parenteral administration. Finally, as demonstrated in our *in vitro* experiments, it did not cause cell toxicity up to 10μM, a concentration ~10^4-fold higher than the calculated EC_{50}.

In addition to these pharmacological properties, neurounina-1 exerted a remarkable neuroprotective effect in both *in vitro* and in *in vivo* experimental models of cerebral ischemia possibly by enhancing NCX activity. In particular, cortical neurons exposed to neurounina-1 displayed a higher resistance to neuronal damage induced by 3h of OGD or 3h of OGD followed by 21h of reoxygenation as compared to vehicle-treated neurons. It is possible to hypothesize that part of this neuroprotective effect of neurounina-1 during OGD followed by reoxygenation is due to the increase in NCX activity that, in turn, counteracts ER-Ca^{2+} depletion occurring in neurons during OGD followed by reoxygenation, a mechanism mediated by NCX1 isoform (Sirabella et al., 2009).

Interestingly, the results obtained *in vivo* showed that the intraperitoneal administration of neurounina-1 in single doses ranging from 0.003 to 30μg/kg significantly reduced the infarct volume in a mouse model of tMCAO. Remarkably, neurounina-1 was effective even

Molecular Pharmacology Fast Forward. Published on October 11, 2012 as DOI: 10.1124/mol.112.080986
This article has not been copyedited and formatted. The final version may differ from this version.

when administered up to 5h after ischemia induction, a therapeutic window that, along with its viable route of administration, may have interesting clinical perspectives.

Since neurounina-1 contains a benzodiazepine-like structure, we tested whether it activates the $GABA_A$-mediated currents, whose increase might interfere with the ischemic process. Indeed, neurounina-1 in the presence of GABA increased chloride currents in a concentration-dependent manner with an EC_{50} of 3.6nM. In addition, the effect of neurounina-1 on GABA-induced chloride currents was completely reverted by flumazenil, the competitive antagonist of the benzodiazepine recognition site on $GABA_A$-receptor. However, although neurounina-1 reinforced the action of GABA on $GABA_A$ receptor, at the same time it reduced its release. In consideration of this dual and opposite action of neurounina-1 on GABA neurotransmission, we can hypothesize that the modulation of GABA transmission might play a less relevant role in the neuroprotective effect exerted by neurounina-1 after cerebral ischemia. In accordance with this hypothesis, the administration of flumazenil in ischemic mice did not revert the neuroprotective effect of neurounina-1.

Another aspect that deserves consideration is the effect of neurounina-1 on glutamate release from cortical synaptosomes that suggested that part of the neuroprotective effect of the newly synthesized compound in stroke could be due to a partial inhibition of both endogenous glutamate release and NMDA-receptor activity. Although this hypothesis cannot be ruled out by the results of *in vitro* experiments, it should be considered that a large body of evidence produced in the last 20 years showed that glutamate-receptor antagonists may be effective as neuroprotectants only if administered before or immediately after middle cerebral artery occlusion in rodents. In fact, the efficacy of these compounds is lost when administered one hour after stroke onset (Buchan et al.,1991;Di Renzo et al.,2009;Gladstone et al.,2002;Hossmann,1996). By contrast, in our study

Molecular Pharmacology Fast Forward. Published on October 11, 2012 as DOI: 10.1124/mol.112.080986
This article has not been copyedited and formatted. The final version may differ from this version.

neurounina-1 is also effective when administered 5 hours after stroke onset. It should be also considered that NMDA receptor antagonists exert part of their neuroprotective effect in stroke animal models by their hypothermic effect (Buchan and Pulsinelli,1990), whereas in the present study neurounina-1 did not affect body temperature.

At variance with the results of the present study, some data present in the literature showed that a pharmacological inhibition of NCX activity protects brain against stroke (Jeffs et al.,2007). However, it has also been demonstrated that these drugs are not selective for NCX (Annunziato et al.,2004;Pintado et al.,2000;Reuter et al.,2002) and some of them possess a remarkable and long-lasting hypothermic effect (Pignataro et al.,2004b) that is neuroprotective by itself.

As concern the possibility that neurounina-1 administration might affect cardiac function, it is difficult to predict neurounina-1 effect on the cardiovascular system for the controversial role played by NCX1.1 in the heart under different pathophysiological conditions. In fact, some reports suggest that elevated NCX1 activity might be associated to heart failure and to arrhythmia, whereas other reports indicate that the overexpression of NCX1 or an increase of its activity results in an attenuation of postinfarction myocardial dysfunction and a preserved diastolic function (Hasenfuss et al.,1999;Litwin and Bridge,1997;Min et al.,2002;Sipido et al.,2002). Although future and more specific studies are necessary to evaluate the action after acute, subacute and chronic regimens of neurounina-1 on all the cardiovascular functions, we found that after 1 and 7 days of administration of this NCX1-2 activator, no increase in mortality rate was observed, either in mice that underwent to cerebral ischemia or in sham operated animals.

Collectively, our results showed that neurounina-1 is provided with high potency for NCX1 and NCX2, high lipophilicity index, low toxicity, and a remarkable neuroprotective effect in

Molecular Pharmacology Fast Forward. Published on October 11, 2012 as DOI: 10.1124/mol.112.080986
This article has not been copyedited and formatted. The final version may differ from this version.

experimental model of cerebral ischemia with a wide therapeutic window and easy route of administration.

Authorship Contributions

Participated in research design: Annunziato, Bonanno, Caliendo, Cantile, Cuomo, Di Renzo, Fiorino, Gatta, Milanese, Molinaro, Pannaccione, Pignataro, Robello, Santagata, Scorziello, Secondo, Severino

Conducted experiments: Ambrosino, Cantile, Cuomo, Fiorino, Gatta, Milanese, Molinaro, Pannaccione, Scorziello, Secondo, Severino, Sisalli

Contributed new reagents or analytic tools:

Performed data analysis: Ambrosino, Cantile, Cuomo, Fiorino, Gatta, Milanese, Molinaro, Pannaccione, Secondo, Severino, Sisalli

Wrote or contributed to the writing of the manuscript: Annunziato, Bonanno, Cantile, Cuomo, Di Renzo, Milanese, Molinaro, Pannaccione, Pignataro, Secondo

REFERENCES

Annunziato L, Cataldi M, Pignataro G, Secondo A and Molinaro P (2007) Glutamate-independent calcium toxicity: introduction. *Stroke* **38**(2 Suppl):661-664.

Annunziato L, Molinaro P, Secondo A, Panaccione A, Scorziello A, Pignataro G, Cuomo O, Sirabella R, Boscia F, Spinali A and Di Renzo G (2009) *The Na+/Ca2+ Exchanger: A Target for Therapeutic Intervention in Cerebral Ischemia*. Humana Press.

Annunziato L, Pignataro G and Di Renzo GF (2004) Pharmacology of brain Na+/Ca2+ exchanger: from molecular biology to therapeutic perspectives. *Pharmacol Rev* **56**(4):633-654.

Blaustein MP and Lederer WJ (1999) Sodium/calcium exchange: its physiological implications. *Physiol Rev* **79**(3):763-854.

Brogden RN and Goa KL (1988) Flumazenil. A preliminary review of its benzodiazepine antagonist properties, intrinsic activity and therapeutic use. *Drugs* **35**(4):448-467.

Buchan A, Li H and Pulsinelli WA (1991) The N-methyl-D-aspartate antagonist, MK-801, fails to protect against neuronal damage caused by transient, severe forebrain ischemia in adult rats. *J Neurosci* **11**(4):1049-1056.

Buchan A and Pulsinelli WA (1990) Hypothermia but not the N-methyl-D-aspartate antagonist, MK-801, attenuates neuronal damage in gerbils subjected to transient global ischemia. *J Neurosci* **10**(1):311-316.

Craner MJ, Newcombe J, Black JA, Hartle C, Cuzner ML and Waxman SG (2004) Molecular changes in neurons in multiple sclerosis: altered axonal expression of

Nav1.2 and Nav1.6 sodium channels and Na+/Ca2+ exchanger. *Proc Natl Acad Sci U S A* **101**(21):8168-8173.

Cuomo O, Gala R, Pignataro G, Boscia F, Secondo A, Scorziello A, Pannaccione A, Viggiano D, Adornetto A, Molinaro P, Li XF, Lytton J, Di Renzo G and Annunziato L (2008) A critical role for the potassium-dependent sodium-calcium exchanger NCKX2 in protection against focal ischemic brain damage. *J Neurosci* **28**(9):2053-2063.

Cuomo O, Pignataro G, Gala R, Scorziello A, Gravino E, Piazza O, Tufano R, Di Renzo G and Annunziato L (2007) Antithrombin reduces ischemic volume, ameliorates neurologic deficits, and prolongs animal survival in both transient and permanent focal ischemia. *Stroke* **38**(12):3272-3279.

Di Renzo G, Pignataro G and Annunziato L (2009) *Why have Ionotropic and Metabotropic Glutamate Antagonists Failed in Stroke Therapy?* Springer.

Eriksson KS, Stevens DR and Haas HL (2001) Serotonin excites tuberomammillary neurons by activation of Na(+)/Ca(2+)-exchange. *Neuropharmacology* **40**(3):345-351.

Fameli N, van Breemen C and Kuo KH (2007) A quantitative model for linking Na+/Ca2+ exchanger to SERCA during refilling of the sarcoplasmic reticulum to sustain [Ca2+] oscillations in vascular smooth muscle. *Cell Calcium* **42**(6):565-575.

Formisano L, Saggese M, Secondo A, Sirabella R, Vito P, Valsecchi V, Molinaro P, Di Renzo G and Annunziato L (2008) The two isoforms of the Na+/Ca2+ exchanger, NCX1 and NCX3, constitute novel additional targets for the prosurvival action of Akt/protein kinase B pathway. *Mol Pharmacol* **73**(3):727-737.

Gladstone DJ, Black SE, Hakim AM, Heart and Stroke Foundation of Ontario Centre of Excellence in Stroke R (2002) Toward wisdom from failure: lessons from

neuroprotective stroke trials and new therapeutic directions. *Stroke* **33**(8):2123-2136.

Grynkiewicz G, Poenie M and Tsien RY (1985) A new generation of Ca2+ indicators with greatly improved fluorescence properties. *J Biol Chem* **260**(6):3440-3450.

Gupta MP, Makino N, Khatter K and Dhalla NS (1986) Stimulation of Na+-Ca2+ exchange in heart sarcolemma by insulin. *Life Sci* **39**(12):1077-1083.

Hasegawa H, Muraoka M, Matsui K and Kojima A (2003) Discovery of a novel potent Na+/Ca2+ exchanger inhibitor: design, synthesis and structure-activity relationships of 3,4-dihydro-2(1H)-quinazolinone derivatives. *Bioorg Med Chem Lett* **13**(20):3471-3475.

Hasenfuss G, Schillinger W, Lehnart SE, Preuss M, Pieske B, Maier LS, Prestle J, Minami K and Just H (1999) Relationship between Na+-Ca2+-exchanger protein levels and diastolic function of failing human myocardium. *Circulation* **99**(5):641-648.

Hossmann KA (1996) Excitotoxic mechanisms in focal ischemia. *Advances in neurology* **71**:69-74.

Iwamoto T, Inoue Y, Ito K, Sakaue T, Kita S and Katsuragi T (2004a) The exchanger inhibitory peptide region-dependent inhibition of Na+/Ca2+ exchange by SN-6 [2-[4-(4-nitrobenzyloxy)benzyl]thiazolidine-4-carboxylic acid ethyl ester], a novel benzyloxyphenyl derivative. *Mol Pharmacol* **66**(1):45-55.

Iwamoto T and Kita S (2006) YM-244769, a novel Na+/Ca2+ exchange inhibitor that preferentially inhibits NCX3, efficiently protects against hypoxia/reoxygenation-induced SH-SY5Y neuronal cell damage. *Mol Pharmacol* **70**(6):2075-2083.

Iwamoto T, Kita S, Uehara A, Imanaga I, Matsuda T, Baba A and Katsuragi T (2004b) Molecular determinants of Na+/Ca2+ exchange (NCX1) inhibition by SEA0400. *J Biol Chem* **279**(9):7544-7553.

Iwamoto T, Kita S, Uehara A, Inoue Y, Taniguchi Y, Imanaga I and Shigekawa M (2001) Structural domains influencing sensitivity to isothiourea derivative inhibitor KB-R7943 in cardiac Nna(+)/Ca(2+) exchanger. *Mol Pharmacol* **59**(3):524-531.

Iwamoto T, Uehara A, Nakamura TY, Imanaga I and Shigekawa M (1999) Chimeric analysis of Na(+)/Ca(2+) exchangers NCX1 and NCX3 reveals structural domains important for differential sensitivity to external Ni(2+) or Li(+). *J Biol Chem* **274**(33):23094-23102.

Iwamoto T, Wakabayashi S, Imagawa T and Shigekawa M (1998) Na+/Ca2+ exchanger overexpression impairs calcium signaling in fibroblasts: inhibition of the [Ca2+] increase at the cell periphery and retardation of cell adhesion. *Eur J Cell Biol* **76**(3):228-236.

Iwamoto T, Watano T and Shigekawa M (1996) A novel isothiourea derivative selectively inhibits the reverse mode of Na+/Ca2+ exchange in cells expressing NCX1. *J Biol Chem* **271**(37):22391-22397.

Jeffs GJ, Meloni BP, Bakker AJ and Knuckey NW (2007) The role of the Na(+)/Ca(2+) exchanger (NCX) in neurons following ischaemia. *J Clin Neurosci* **14**(6):507-514.

Jeon D, Chu K, Jung KH, Kim M, Yoon BW, Lee CJ, Oh U and Shin HS (2008) Na(+)/Ca(2+) exchanger 2 is neuroprotective by exporting Ca(2+) during a transient focal cerebral ischemia in the mouse. *Cell Calcium* **43**(5):482-491.

Ketelaars SO, Gorter JA, Aronica E and Wadman WJ (2004) Calcium extrusion protein expression in the hippocampal formation of chronic epileptic rats after kainate-induced status epilepticus. *Epilepsia* **45**(10):1189-1201.

Litwin SE and Bridge JH (1997) Enhanced Na(+)-Ca2+ exchange in the infarcted heart. Implications for excitation-contraction coupling. *Circ Res* **81**(6):1083-1093.

Makino N, Zhao D and Dhalla NS (1988) Stimulation of heart sarcolemmal Na+-Ca2+ exchange by concanavalin A. *Biochem Biophys Res Commun* **154**(1):245-251.

Matsuda T, Arakawa N, Takuma K, Kishida Y, Kawasaki Y, Sakaue M, Takahashi K, Takahashi T, Suzuki T, Ota T, Hamano-Takahashi A, Onishi M, Tanaka Y, Kameo K and Baba A (2001) SEA0400, a novel and selective inhibitor of the Na+-Ca2+ exchanger, attenuates reperfusion injury in the in vitro and in vivo cerebral ischemic models. *J Pharmacol Exp Ther* **298**(1):249-256.

Min JY, Sullivan MF, Yan X, Feng X, Chu V, Wang JF, Amende I, Morgan JP, Philipson KD and Hampton TG (2002) Overexpression of Na+/Ca2+ exchanger gene attenuates postinfarction myocardial dysfunction. *Am J Physiol Heart Circ Physiol* **283**(6):H2466-2471.

Molinaro P, Cuomo O, Pignataro G, Boscia F, Sirabella R, Pannaccione A, Secondo A, Scorziello A, Adornetto A, Gala R, Viggiano D, Sokolow S, Herchuelz A, Schurmans S, Di Renzo G and Annunziato L (2008) Targeted disruption of Na+/Ca2+ exchanger 3 (NCX3) gene leads to a worsening of ischemic brain damage. *J Neurosci* **28**(5):1179-1184.

Molinaro P, Viggiano D, Nistico R, Sirabella R, Secondo A, Boscia F, Pannaccione A, Scorziello A, Mehdawy B, Sokolow S, Herchuelz A, Di Renzo GF and Annunziato L (2011) Na+-Ca2+ Exchanger (NCX3) Knock-Out Mice Display an Impairment in Hippocampal Long-Term Potentiation and Spatial Learning and Memory. *J Neurosci* **31**(20):7312-7321.

Nicoll DA, Hryshko LV, Matsuoka S, Frank JS and Philipson KD (1996) Mutation of amino acid residues in the putative transmembrane segments of the cardiac sarcolemmal Na+-Ca2+ exchanger. *J Biol Chem* **271**(23):13385-13391.

Nicoll DA, Ottolia M, Lu L, Lu Y and Philipson KD (1999) A new topological model of the cardiac sarcolemmal Na+-Ca2+ exchanger. *J Biol Chem* **274**(2):910-917.

Ottolia M, Schumann S, Nicoll DA and Philipson KD (2002) Activation of the cardiac Na+/Ca2+ exchanger by DEPC. *Ann N Y Acad Sci* **976**:85-88.

Pannaccione A, Secondo A, Molinaro P, D'Avanzo C, Cantile M, Esposito A, Boscia F, Scorziello A, Sirabella R, Di Renzo G and Annunziato L (2012) A New Concept: Abeta1-42 Generates a Hyperfunctional Proteolytic NCX3 Fragment That Delays Caspase-12 Activation and Neuronal Death. *J Neurosci* **32**(31):10609-10617.

Philipson KD and Nicoll DA (2000) Sodium-calcium exchange: a molecular perspective. *Annu Rev Physiol* **62**:111-133.

Pignataro G, Gala R, Cuomo O, Tortiglione A, Giaccio L, Castaldo P, Sirabella R, Matrone C, Canitano A, Amoroso S, Di Renzo G and Annunziato L (2004a) Two sodium/calcium exchanger gene products, NCX1 and NCX3, play a major role in the development of permanent focal cerebral ischemia. *Stroke* **35**(11):2566-2570.

Pignataro G, Tortiglione A, Scorziello A, Giaccio L, Secondo A, Severino B, Santagada V, Caliendo G, Amoroso S, Di Renzo G and Annunziato L (2004b) Evidence for a protective role played by the Na+/Ca2+ exchanger in cerebral ischemia induced by middle cerebral artery occlusion in male rats. *Neuropharmacology* **46**(3):439-448.

Pintado AJ, Herrero CJ, Garcia AG and Montiel C (2000) The novel Na(+)/Ca(2+) exchange inhibitor KB-R7943 also blocks native and expressed neuronal nicotinic receptors. *Br J Pharmacol* **130**(8):1893-1902.

Quednau BD, Nicoll DA and Philipson KD (1997) Tissue specificity and alternative splicing of the Na+/Ca2+ exchanger isoforms NCX1, NCX2, and NCX3 in rat. *Am J Physiol* **272**(4 Pt 1):C1250-1261.

Reeves JP, Bailey CA and Hale CC (1986) Redox modification of sodium-calcium exchange activity in cardiac sarcolemmal vesicles. *J Biol Chem* **261**(11):4948-4955.

Reuter H, Henderson SA, Han T, Matsuda T, Baba A, Ross RS, Goldhaber JI and Philipson KD (2002) Knockout mice for pharmacological screening: testing the specificity of Na+-Ca2+ exchange inhibitors. *Circ Res* **91**(2):90-92.

Robello M, Amico C and Cupello A (1993) Regulation of GABAA receptor in cerebellar granule cells in culture: differential involvement of kinase activities. *Neuroscience* **53**(1):131-138.

Scorziello A, Santillo M, Adornetto A, Dell'aversano C, Sirabella R, Damiano S, Canzoniero LM, Renzo GF and Annunziato L (2007) NO-induced neuroprotection in ischemic preconditioning stimulates mitochondrial Mn-SOD activity and expression via Ras/ERK1/2 pathway. *J Neurochem* **103**(4):1472-1480.

Secondo A, Molinaro P, Pannaccione A, Esposito A, Cantile M, Lippiello P, Sirabella R, Iwamoto T, Di Renzo G and Annunziato L (2011) Nitric oxide stimulates NCX1 and NCX2 but inhibits NCX3 isoform by three distinct molecular determinants. *Mol Pharmacol* **79**(3):558-568.

Secondo A, Pannaccione A, Molinaro P, Ambrosino P, Lippiello P, Esposito A, Cantile M, Khatri PR, Melisi D, Di Renzo G and Annunziato L (2009) Molecular pharmacology of the amiloride analog 3-amino-6-chloro-5-[(4-chloro-benzyl)amino]-n-[[(2,4-dimethylbenzyl)-amino]iminomethyl]-pyrazinecarboxamide (CB-DMB) as a pan inhibitor of the Na+-Ca2+ exchanger isoforms NCX1, NCX2, and NCX3 in stably transfected cells. *J Pharmacol Exp Ther* **331**(1):212-221.

Secondo A, Staiano RI, Scorziello A, Sirabella R, Boscia F, Adornetto A, Valsecchi V, Molinaro P, Canzoniero LM, Di Renzo G and Annunziato L (2007) BHK cells transfected with NCX3 are more resistant to hypoxia followed by reoxygenation

than those transfected with NCX1 and NCX2: Possible relationship with mitochondrial membrane potential. *Cell Calcium* **42**(6):521-535.

Sipido KR, Volders PG, Vos MA and Verdonck F (2002) Altered Na/Ca exchange activity in cardiac hypertrophy and heart failure: a new target for therapy? *Cardiovasc Res* **53**(4):782-805.

Sirabella R, Secondo A, Pannaccione A, Scorziello A, Valsecchi V, Adornetto A, Bilo L, Di Renzo G and Annunziato L (2009) Anoxia-induced NF-kappaB-dependent upregulation of NCX1 contributes to Ca2+ refilling into endoplasmic reticulum in cortical neurons. *Stroke* **40**(3):922-929.

Stengl M, Mubagwa K, Carmeliet E and Flameng W (1998) Phenylephrine-induced stimulation of Na+/Ca2+ exchange in rat ventricular myocytes. *Cardiovasc Res* **38**(3):703-710.

Stigliani S, Zappettini S, Raiteri L, Passalacqua M, Melloni E, Venturi C, Tacchetti C, Diaspro A, Usai C and Bonanno G (2006) Glia re-sealed particles freshly prepared from adult rat brain are competent for exocytotic release of glutamate. *J Neurochem* **96**(3):656-668.

Tardito D, Milanese M, Bonifacino T, Musazzi L, Grilli M, Mallei A, Mocaer E, Gabriel-Gracia C, Racagni G, Popoli M and Bonanno G (2010) Blockade of stress-induced increase of glutamate release in the rat prefrontal/frontal cortex by agomelatine involves synergy between melatonergic and 5-HT2C receptor-dependent pathways. *BMC Neurosci* **11**:68.

Watano T, Harada Y, Harada K and Nishimura N (1999) Effect of Na+/Ca2+ exchange inhibitor, KB-R7943 on ouabain-induced arrhythmias in guinea-pigs. *Br J Pharmacol* **127**(8):1846-1850.

Woo SH and Morad M (2001) Bimodal regulation of Na(+)--Ca(2+) exchanger by beta-adrenergic signaling pathway in shark ventricular myocytes. *Proc Natl Acad Sci U S A* **98**(4):2023-2028.

Molecular Pharmacology Fast Forward. Published on October 11, 2012 as DOI: 10.1124/mol.112.080986
This article has not been copyedited and formatted. The final version may differ from this version.

FOOTNOTES

We thank Dr Paola Merolla for editorial revision and Vincenzo Grillo and Carmine Capitale for technical assistance. This work was supported by Ministero della Salute “Ricerca Finalizzata 2006”, “Ricerca Oncologica 2006”, “Progetto Strategico 2007”, “Progetto Ordinario 2007”, and “Ricerca Finalizzata 2009” [Grants RF-FSL-352059, RF-IDI-2006-367185, RF-06711, RF-SDN-2007-666932, RF-0832]; and Ministero dell’Istruzione, dell’Università e della Ricerca “Programma Operativo Nazionale” and “COFIN2008” [Grants PON_01602, 20089BARSR_002]; all to LA.

P.M., M.C., O.C. contributed equally to this paper

Neurounina-1 is under patent protection (FI2010A000233) obtained from Italian Office for Patents and Trademarks of the Ministry of Industry and Trade.

Molecular Pharmacology Fast Forward. Published on October 11, 2012 as DOI: 10.1124/mol.112.080986
This article has not been copyedited and formatted. The final version may differ from this version.

FIGURE LEGENDS

Fig. 1. Effect of neurounina-1 on NCX1, NCX2 and NCX3 activity measured by Na^+-dependent $^{45}Ca^{2+}$ influx/efflux and Fura-2 monitored Ca^{2+} techniques. Inset shows the chemical structure of neurounina-1. **A** and **B**, concentration-response curves of the effects of neurounina-1 on Na_o-dependent $^{45}Ca^{2+}$ efflux and Na_o-dependent $^{45}Ca^{2+}$ uptake, respectively, in BHK cells expressing NCX1, NCX2, or NCX3. **C**, Effect of neurounina-1 (0.0001-0.01μM) on NCX1, NCX2, and NCX3 activity measured by single-cell Fura-2AM microfluorimetry (n=60 cells for each group). Data are calculated as Δ% of plateau/basal $[Ca^{2+}]_i$ values after Na^+-free addition. Under control conditions, basal values of $[Ca^{2+}]_i$ were (in nM): 72±4.8 in BHK-NCX1 cells, 79±3.5 in BHKNCX2 cells, and 73±4.2 in BHK-NCX3 cells. Data are means ± S.E.M. of three independent experiments. *, $p < 0.05$ versus NCX3 and control groups. **, $p < 0.05$ versus NCX2 and NCX3 groups.

Fig. 2. Effect of neurounina-1 on NCX1, NCX2, and NCX3 currents measured by patch-clamp technique in whole cell configuration. In **A, B,** and **C,** the left panels represent superimposed traces of total currents recorded from BHK cells stably transfected with NCX1, NCX2, or NCX3, respectively, without (grey trace) or with Ni^{2+} (black trace); the middle panels show representative traces of NCX1, NCX2, and NCX3 isolated Ni^{2+}-subtracted currents under control conditions, in the presence of neurounina-1 or after wash; the right panels show concentration-response curves of the neurounina-1 effect on NCX1 (top) and NCX2 (bottom) currents. **D,** representative superimposed traces of the currents recorded from BHK wild-type under control conditions (grey traces) and after 10 nM neurounina-1 exposure (black traces). **E,** quantification of neurounina-1 effect (10 nM) on NCX1, NCX2, and NCX3 currents in the reverse and forward modes of operation. The

Molecular Pharmacology Fast Forward. Published on October 11, 2012 as DOI: 10.1124/mol.112.080986
This article has not been copyedited and formatted. The final version may differ from this version.

values are expressed as percentage mean ± S.E.M. of 3 independent experimental sessions (n=20 for each group). *p < 0.05 versus the respective control groups.

Fig. 3. Effect of neurounina-1 on NCX1/NCX3 chimeras measured by Na^+_o-dependent $^{45}Ca^{2+}$ uptake and $^{45}Ca^{2+}$ efflux techniques. On the left of the figure, all chimeras have been reported as cartoons. **A** and **B**, effect of 10 nM neurounina-1 on NCX1/NCX3 chimeras measured by Na^+_o-dependent $^{45}Ca^{2+}$ efflux (panel A) and uptake (panel B). Values are expressed as percentage versus the respective control. Data are means ± S.E.M. of six independent experiments. *, p < 0.05 versus the respective control group. **, p < 0.05 versus the respective control and NCX1WT groups.

Fig. 4. Effect of neurounina-1 on NCX1 mutants measured by Na^+_o-dependent $^{45}Ca^{2+}$ uptake and Fura-2 single-cell microfluorimetry. **A**, amino acid alignment of α_1 and α_2 regions of NCX1, NCX2 and NCX3. Conserved amino acids among exchangers are indicated with dots. Asterisks indicate the position of mutations that altered neurounina-1 sensitivity. **B**, effect of neurounina-1 on NCX1 mutants, measured by Na^+_o-dependent $^{45}Ca^{2+}$ uptake, in which the single residues in the regions indicated in panel A were exchanged with the corresponding residue of NCX3. Values are represented as percentage ratio of the values obtained in the presence of 10 nM neurounina-1 versus non-treated control cells. Data are presented as means ± S.E.M. of six independent experiments. *, p < 0.05 versus the respective control group. **, p < 0.05 versus NCX1WT and NCX3WT groups. **C**, Na^+-free induced $[Ca^{2+}]_i$ increase in cells expressing the above described NCX1 mutants and treated with 10 nM neurounina-1. Each value is reported as % of its non-treated controls. Data are presented as means ± S.E.M. of three independent

Molecular Pharmacology Fast Forward. Published on October 11, 2012 as DOI: 10.1124/mol.112.080986
This article has not been copyedited and formatted. The final version may differ from this version.

experiments. *, $p < 0.05$ versus the respective control group. **, $p < 0.05$ versus NCX1WT and NCX3WT groups.

Fig. 5. Effect of neurounina-1 on cell survival. **A**, cell death percentage of BHK cells stably transfected with NCX1, NCX2, or NCX3 exposed to 10 μM neurounina-1 for 24h. **B**, mitochondrial activity of BHK cells exposed to 10 μM neurounina-1 for 24h. **C**, Representative images of the effect of neurounina-1 on cell survival in primary cortical neurons subjected to oxygen and glucose deprivation (OGD) plus reoxygenation (top). Quantification of cell death in normoxia, after 3h OGD and after 3h OGD followed by 21h of reoxygenation, in the presence or in the absence of 10 nM neurounina-1 (Bottom). Data are presented as means ± S.E.M. *, $p < 0.05$ versus the control group. **, $p < 0.05$ versus the respective vehicle-treated group.

Fig. 6. Dose-effect of neurounina-1 on ischemic volume in mice subjected to tMCAO. **A** and **B**, dose-dependent effect of neurounina-1 on the ischemic volume, administered i.p. 3h or 5h after stroke onset, respectively. Each column represents the mean ± S.E.M. of the % of the infarct volume compared to the ipsilateral hemisphere. Each dot represents the single value measured. *, $p < 0.05$ versus control group. **, $p < 0.05$ versus 0.01 μg/kg-treated group.

Fig. 7. Effect of neurounina-1 on $GABA_A$-mediated chloride currents in rat cerebellar granule cells and effect of flumazenil on neurounina-1-induced neuroprotection in ischemic mice. **A** and **B**, representative traces and quantification of chloride currents elicited by 10 μM GABA under control conditions, in the presence of neurounina-1 and in the presence

Molecular Pharmacology Fast Forward. Published on October 11, 2012 as DOI: 10.1124/mol.112.080986
This article has not been copyedited and formatted. The final version may differ from this version.

of both neurounina-1 and flumazenil. *, $p < 0.05$ versus GABA and GABA+neurounina-1+flumazenil groups. **C**, concentration-dependent effect of neurounina-1 on chloride currents evoked by $GABA_A$ receptor exposed to 10 μM GABA. **D**, evaluation of the ischemic volume in mice 24h after tMCAO and treated with three injections of 10 mg/kg flumazenil 3, 4 and 5h after tMCAO and one injection of 30 ng/kg neurounina-1 3h after tMCAO. Each dot represents the single value measured. *, $p < 0.05$ versus vehicle and flumazenil-treated groups.

Fig. 8. Effect of neurounina-1 on endogenous GABA and glutamate release from cortical synaptosomes and on $[Ca^{2+}]_i$ increase elicited by NMDA receptor activation in primary cortical neurons. **A**, endogenous glutamate release from cortical synaptosomes under basal conditions, after 15 mM KCl, in Ca^{2+}-free medium, and in the presence of the glutamate uptake inhibitor DL-TBOA. **B**, effect of different concentrations of neurounina-1 on endogenous glutamate release induced by 15 mM KCl (data were subtracted for basal release values). **C**, 100 μM NMDA-induced $[Ca^{2+}]_i$ increase under control conditions, in the presence of 10 nM neurounina-1 or in the presence of the NMDA receptor blocker, MK-801 (100 μM). **D**, endogenous GABA release from cortical synaptosomes under basal conditions, after 15 mM KCl, in Ca^{2+}-free medium or in the presence of the GABA uptake inhibitor SKF89976A. **E**, effect of different concentrations of neurounina-1 on endogenous GABA release induced by 15 mM KCl (data were subtracted for basal release values). *, $p < 0.05$ versus the control group; **, $p < 0.05$ versus 10 nM neurounina-1; #, $p < 0.05$ versus control and Ca^{2+}-free groups.

Molecular Pharmacology Fast Forward. Published on October 11, 2012 as DOI: 10.1124/mol.112.080986
This article has not been copyedited and formatted. The final version may differ from this version.

Table 1 Effects of neurounina-1 on endogenous glutamate and GABA basal release. Neurounina-1 at a concentration ranging from 10 to 100 nM did not affect basal release of the endogenous glutamate and GABA neurotransmitters.

Neurounina-1 (nM)	Endogenous glutamate basal release (pmol/mg prt) Mean (± SEM)	Endogenous GABA basal release (pmol/mg prt) Mean (± SEM)	n
0	92.2 ± 10.78	42.50 ± 4.66	10
10	80.1 ± 15.21	45.41 ± 6.43	10
30	83.2 ± 8.06	44.50 ± 4.90	10
100	90.1 ± 13.63	45.00 ± 4.58	10

Figure 1

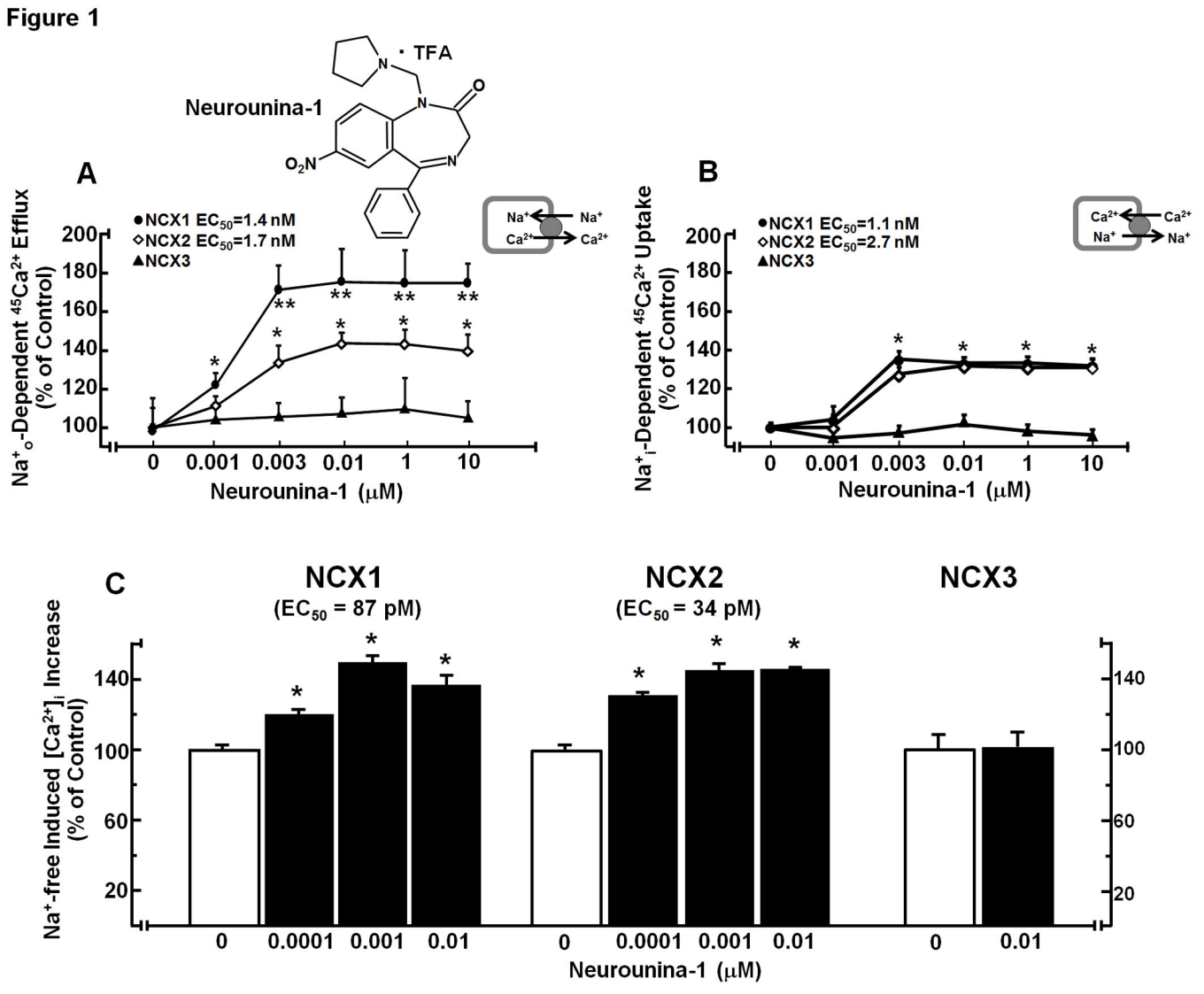
Neurounina-1
· TFA
A
B
C
NCX1
(EC50 = 87 pM)
NCX2
(EC50 = 34 pM)
NCX3
Neurounina-1 (μM)

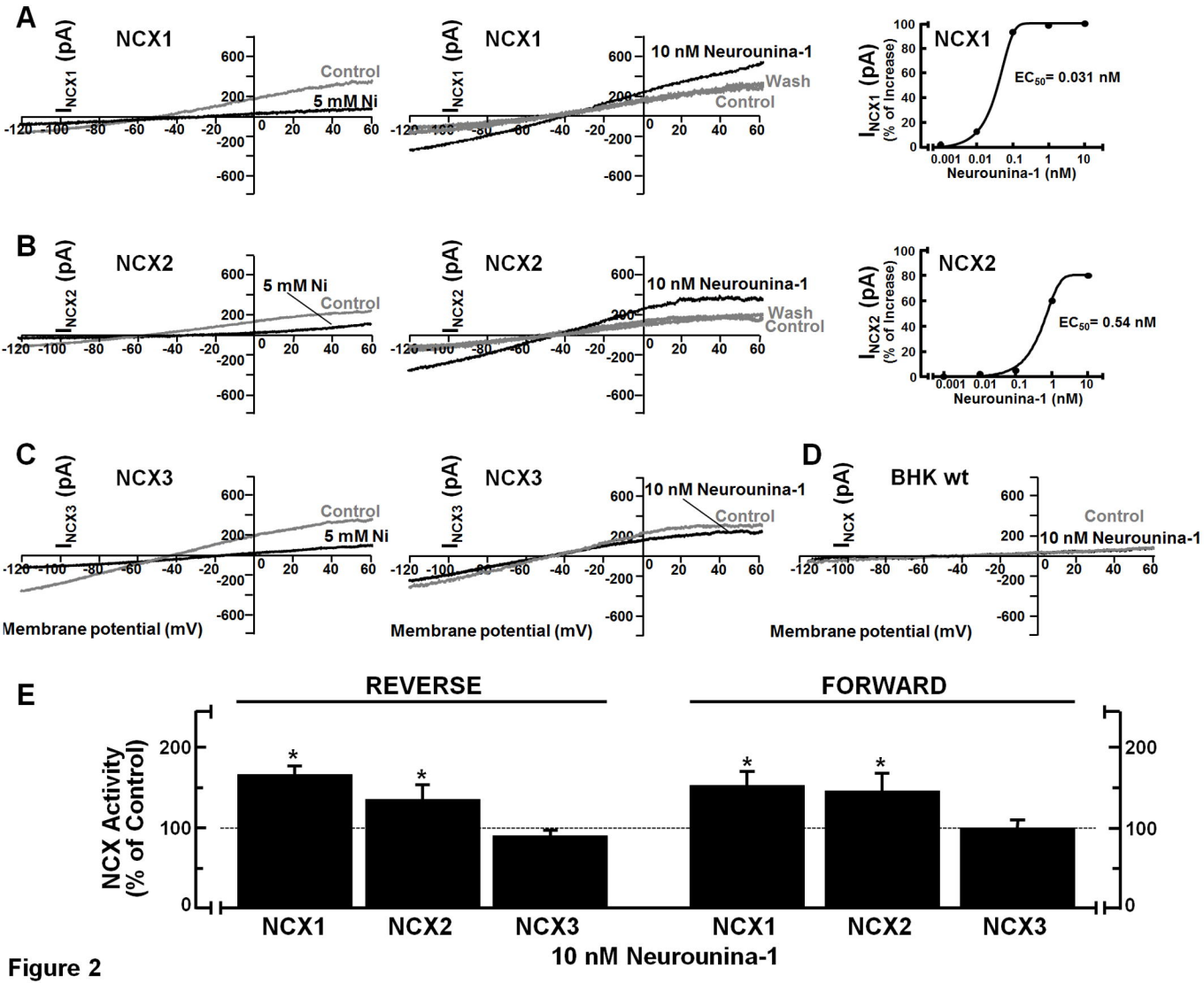
A
NCX1
I_{NCX1} (pA)
Control
5 mM Ni
10 nM Neurounina-1
Wash
Control
EC_{50}= 0.031 nM
I_{NCX1} (% of Increase)
Neurounina-1 (nM)
B
NCX2
I_{NCX2} (pA)
5 mM Ni
Control
10 nM Neurounina-1
Wash
Control
EC_{50}= 0.54 nM
I_{NCX2} (% of Increase)
Neurounina-1 (nM)
C
NCX3
I_{NCX3} (pA)
Control
5 mM Ni
10 nM Neurounina-1
Control
Membrane potential (mV)
D
BHK wt
I_{NCX} (pA)
Control
10 nM Neurounina-1
Membrane potential (mV)
E
REVERSE
FORWARD
NCX Activity (% of Control)
NCX1
NCX2
NCX3
10 nM Neurounina-1

Figure 2

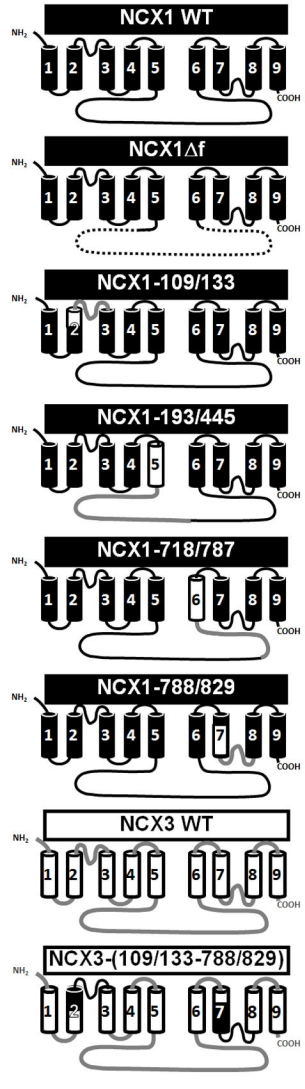
NCX1 WT
NCX1Δf
NCX1-109/133
NCX1-193/445
NCX1-718/787
NCX1-788/829
NCX3 WT
NCX3-(109/133-788/829)
NH2
COOH
1 2 3 4 5 6 7 8 9

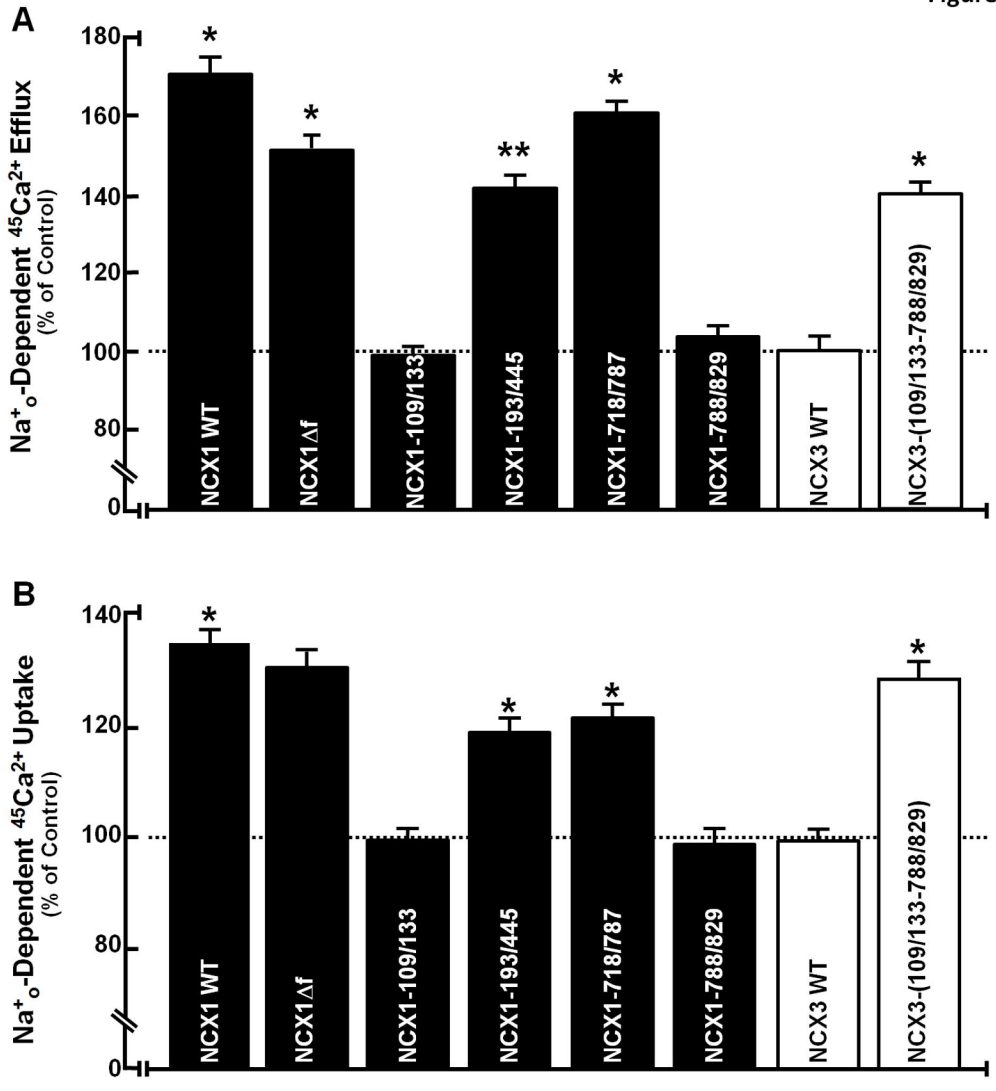
A
Na+o-Dependent 45Ca2+ Efflux
(% of Control)
180
160
140
120
100
80
0
*
*
**
*
*
NCX1 WT
NCX1Δf
NCX1-109/133
NCX1-193/445
NCX1-718/787
NCX1-788/829
NCX3 WT
NCX3-(109/133-788/829)
B
Na+o-Dependent 45Ca2+ Uptake
(% of Control)
140
120
100
80
0
*
*
*
*
NCX1 WT
NCX1Δf
NCX1-109/133
NCX1-193/445
NCX1-718/787
NCX1-788/829
NCX3 WT
NCX3-(109/133-788/829)

Figure 4

A

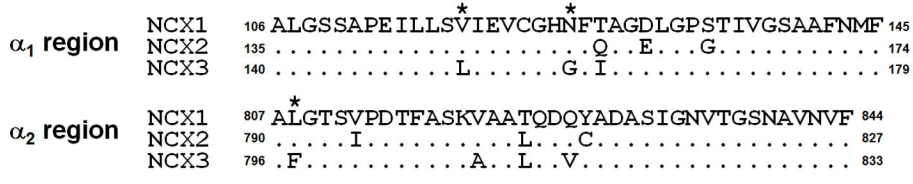
α1 region
NCX1 106 ALGSSAPEILLSVIEVCGHNFTAGDLGPSTIVGSAAFNMF 145
NCX2 135 .....Q..E...G..... 174
NCX3 140 .....L.....G.I..... 179
α2 region
NCX1 807 ALGTSVPDTFASKVAATQDQYADASIGNVTGSNAVNVF 844
NCX2 790 .....I.....L...C..... 827
NCX3 796 .F.....A..L..V..... 833

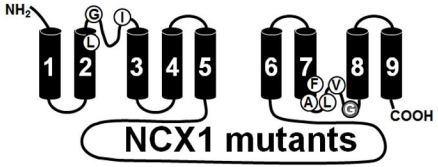
NH2
1
2
3
4
5
6
7
8
9
COOH
NCX1 mutants

B

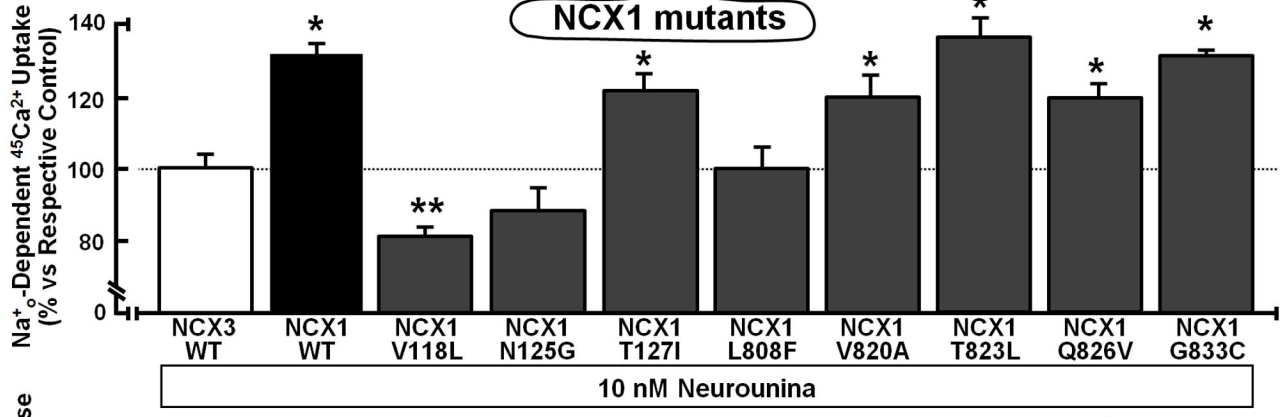
Na+o-Dependent 45Ca2+ Uptake (% vs Respective Control)
140
120
100
80
0
NCX3 WT
NCX1 WT
NCX1 V118L
NCX1 N125G
NCX1 T127I
NCX1 L808F
NCX1 V820A
NCX1 T823L
NCX1 Q826V
NCX1 G833C
10 nM Neurounina

C

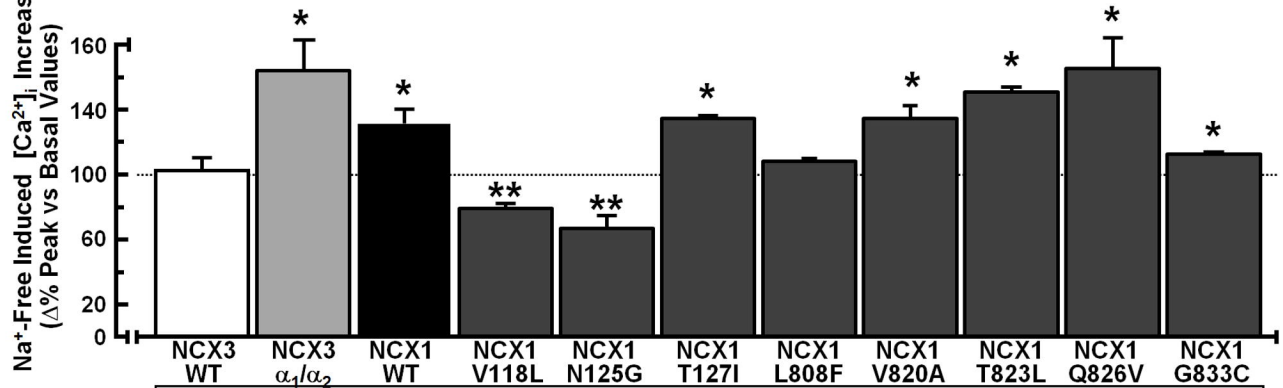
Na+-Free Induced [Ca2+]i Increase (Δ% Peak vs Basal Values)
160
140
100
60
20
0
NCX3 WT
NCX3 α1/α2
NCX1 WT
NCX1 V118L
NCX1 N125G
NCX1 T127I
NCX1 L808F
NCX1 V820A
NCX1 T823L
NCX1 Q826V
NCX1 G833C
10 nM Neurounina

Figure 5

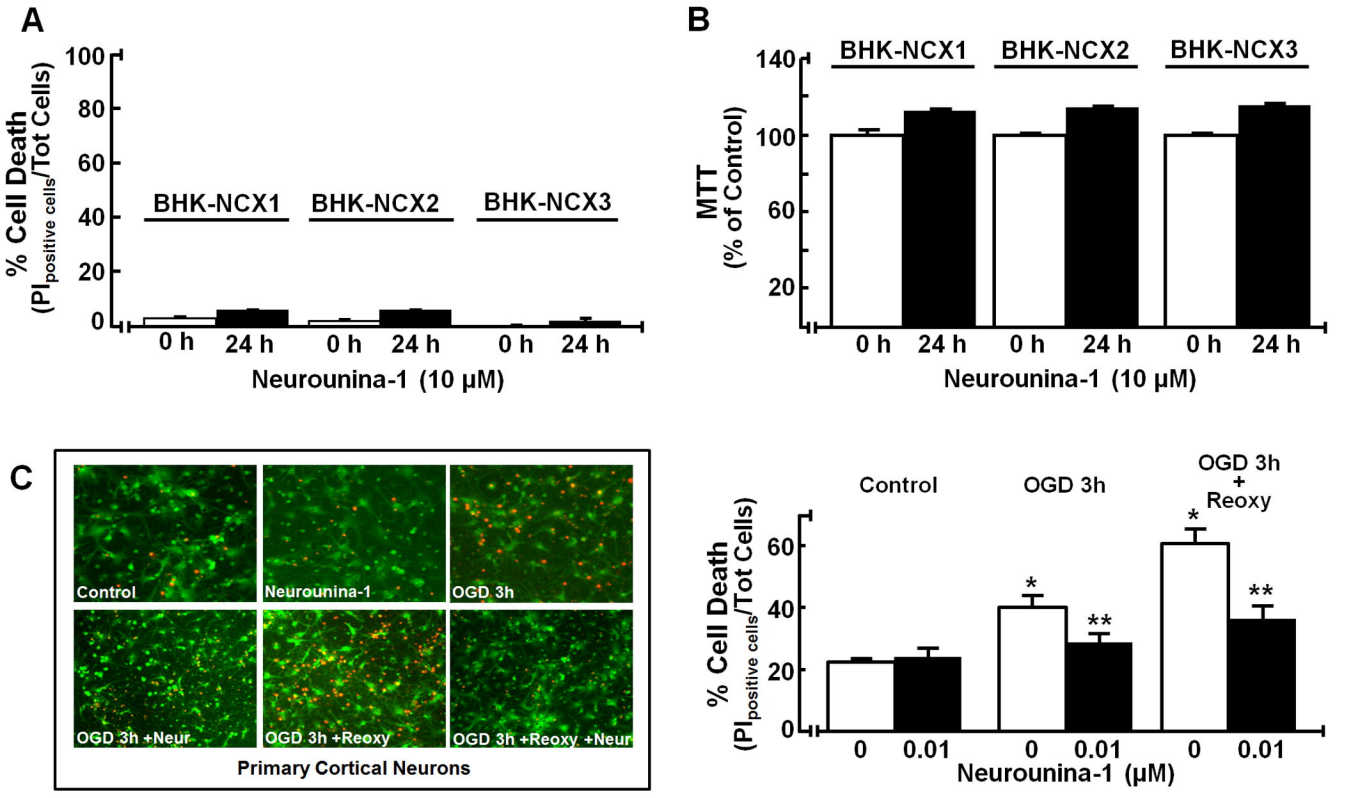
A
% Cell Death
(PI positive cells/Tot Cells)
100
80
60
40
20
0
BHK-NCX1
BHK-NCX2
BHK-NCX3
0 h
24 h
0 h
24 h
0 h
24 h
Neurounina-1 (10 μM)
B
MTT
(% of Control)
140
100
60
20
BHK-NCX1
BHK-NCX2
BHK-NCX3
0 h
24 h
0 h
24 h
0 h
24 h
Neurounina-1 (10 μM)
C
Control
Neurounina-1
OGD 3h
OGD 3h +Neur
OGD 3h +Reoxy
OGD 3h +Reoxy +Neur
Primary Cortical Neurons
Control
OGD 3h
OGD 3h
+
Reoxy
% Cell Death
(PI positive cells/Tot Cells)
60
40
20
0
*
**
*
**
0
0.01
0
0.01
0
0.01
Neurounina-1 (μM)

Figure 6

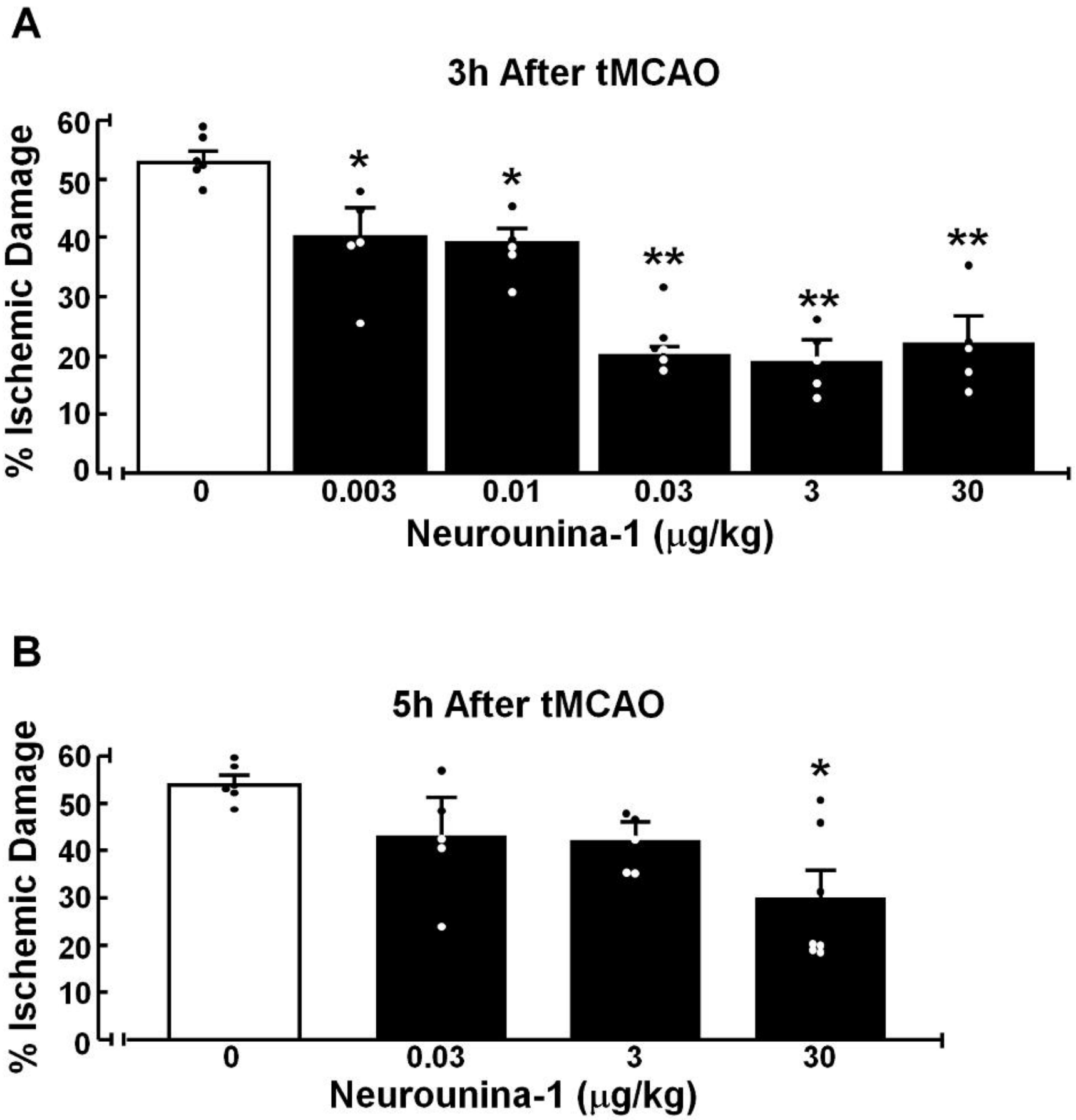
A
3h After tMCAO
% Ischemic Damage
60
50
40
30
20
10
0
*
*
**
**
**
0
0.003
0.01
0.03
3
30
Neurounina-1 (μg/kg)
B
5h After tMCAO
% Ischemic Damage
60
50
40
30
20
10
0
*
0
0.03
3
30
Neurounina-1 (μg/kg)

Figure 7

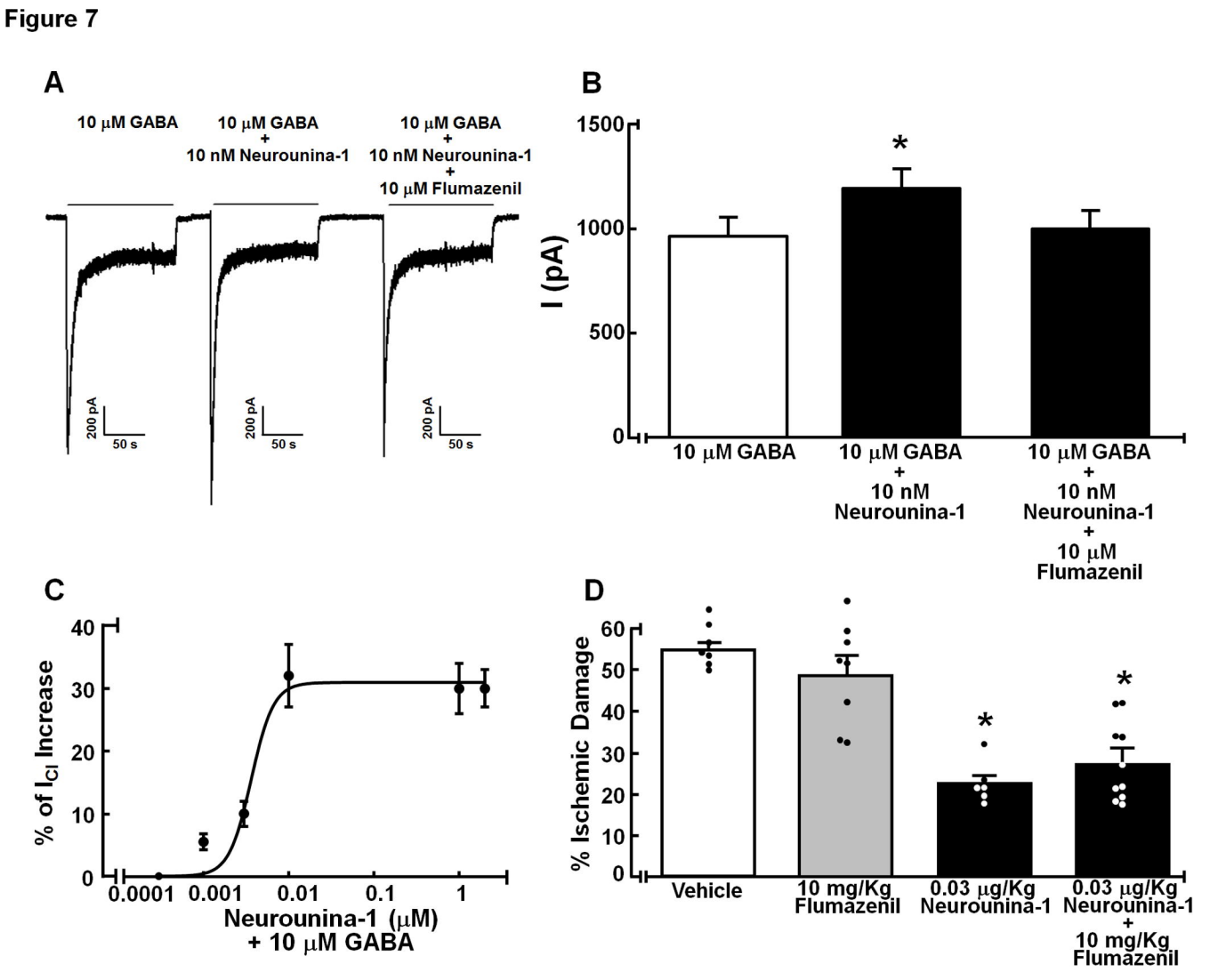
A
10 μM GABA
10 μM GABA + 10 nM Neurounina-1
10 μM GABA + 10 nM Neurounina-1 + 10 μM Flumazenil
200 pA
50 s
B
I (pA)
1500
1000
500
0
*
10 μM GABA
10 μM GABA + 10 nM Neurounina-1
10 μM GABA + 10 nM Neurounina-1 + 10 μM Flumazenil
C
% of I_{Cl} Increase
40
30
20
10
0
0.0001
0.001
0.01
0.1
1
Neurounina-1 (μM) + 10 μM GABA
D
% Ischemic Damage
60
50
40
30
20
10
0
*
*
Vehicle
10 mg/Kg Flumazenil
0.03 μg/Kg Neurounina-1
0.03 μg/Kg Neurounina-1 + 10 mg/Kg Flumazenil

Figure 8

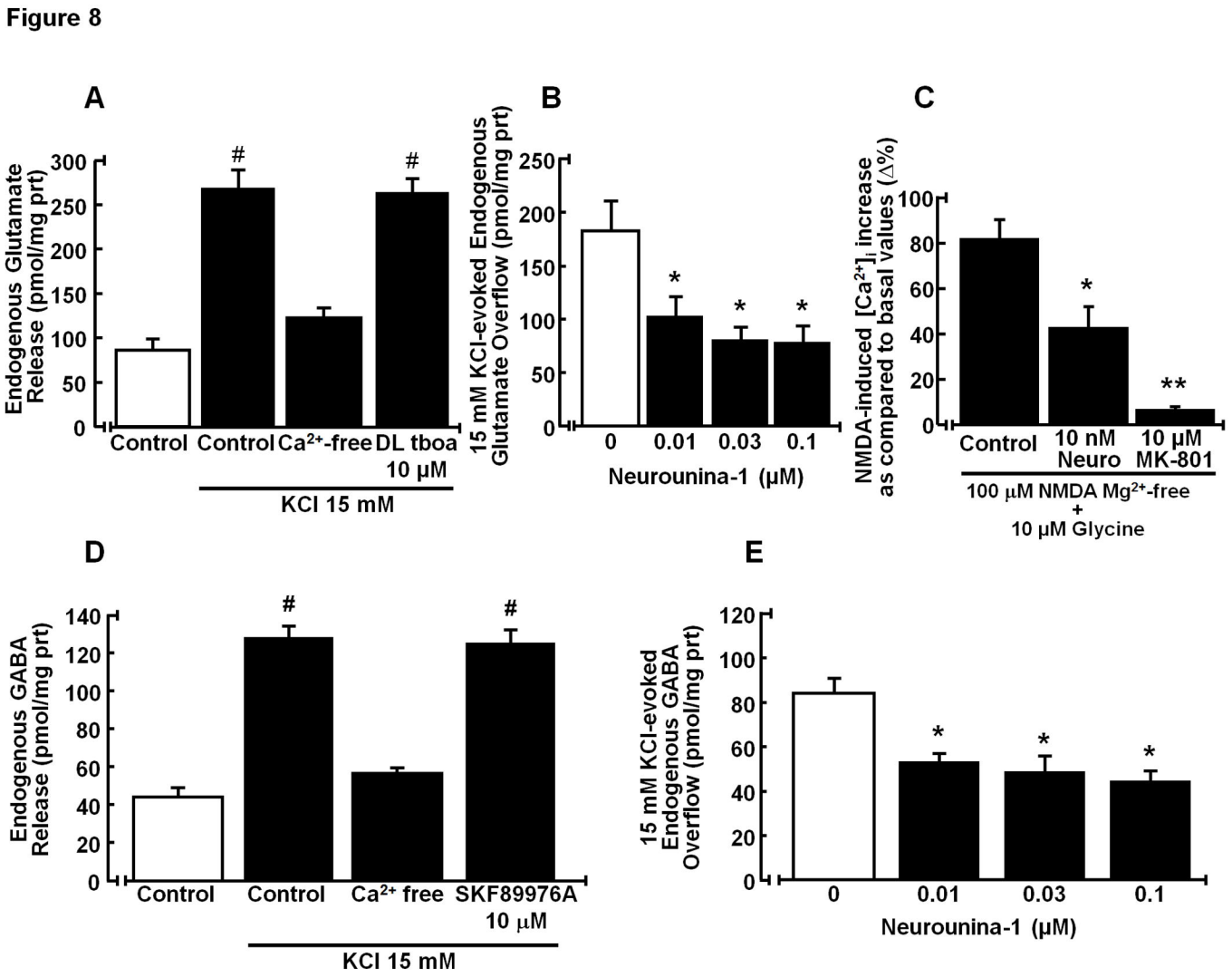
A
Endogenous Glutamate Release (pmol/mg prt)
300
250
200
150
100
50
0
#
#
Control
Control
Ca2+-free
DL tboa 10 μM
KCl 15 mM
B
15 mM KCl-evoked Endogenous Glutamate Overflow (pmol/mg prt)
250
200
150
100
50
0
*
*
*
0
0.01
0.03
0.1
Neurounina-1 (μM)
C
NMDA-induced [Ca2+]i increase as compared to basal values (Δ%)
100
80
60
40
20
0
*
**
Control
10 nM Neuro
10 μM MK-801
100 μM NMDA Mg2+-free
+
10 μM Glycine
D
Endogenous GABA Release (pmol/mg prt)
140
120
100
80
60
40
20
0
#
#
Control
Control
Ca2+ free
SKF89976A 10 μM
KCl 15 mM
E
15 mM KCl-evoked Endogenous GABA Overflow (pmol/mg prt)
120
100
80
60
40
20
0
*
*
*
0
0.01
0.03
0.1
Neurounina-1 (μM)